frontiers in Earth Science

ORIGINAL RESEARCH
published: 29 November 2021
doi: 10.3389/feart.2021.663760

Petrology, Geochemical Characteristics, Tectonic Setting, and Implications for Chromite and PGE Mineralization of the Hongshishan Alaskan-Type Complex in the Beishan Orogenic Collage, North West China

Zhaolin Wang[1,2]*, *Xiaoming Zheng*[3]*, *Guixiang Meng*[1,2], *Hejun Tang*[1,2] and *Tonghui Fang*[3]

[1]Chinese Academy of Geological Sciences, Beijing, China, [2]Deep Exploration Center-SinoProbe Center, China Geological Survey and Chinese Academy of Geological Sciences, Beijing, China, [3]China Non-ferrous Metals Resource Geological Survey, Beijing, China

OPEN ACCESS

Edited by:
David R. Lentz,
University of New Brunswick
Fredericton, Canada

Reviewed by:
Yufeng Deng,
Hefei University of Technology, China
Dongmei Tang,
Institute of Geology and
Geophysics(CAS), China

***Correspondence:**
Zhaolin Wang
wangzl@cags.ac.cn
Xiaoming Zheng
zxm9981@hotmail.com

Specialty section:
This article was submitted to
Economic Geology,
a section of the journal
Frontiers in Earth Science

Received: 03 February 2021
Accepted: 25 October 2021
Published: 29 November 2021

Citation:
Wang Z, Zheng X, Meng G, Tang H and Fang T (2021) Petrology, Geochemical Characteristics, Tectonic Setting, and Implications for Chromite and PGE Mineralization of the Hongshishan Alaskan-Type Complex in the Beishan Orogenic Collage, North West China.
Front. Earth Sci. 9:663760.
doi: 10.3389/feart.2021.663760

The Hongshishan mafic-ultramafic complex is situated in the north of the Beishan orogenic collage and the southern part of the Central Asian Orogenic Belt. This paper outlines the petrological, geochemical, and mineralogical data of the Hongshishan ultramafic–mafic complex in the Beishan orogenic collage to constrain its tectonic setting and mineralization. The lithological units of the complex include dunite, clinopyroxene peridotite, pyroxenite, and gabbro. The complex showed concentric zonation, from clinopyroxene peridotite and dunite in the core to pyroxenite and gabbro in the margin. These ultramafic–mafic rocks are characterized by cumulate and layering textures. Field observations, petrography, and significant elemental composition variation, a decreasing sequence of ferromagnesian minerals (Mg#), olivine Fo, and spinel Cr#, all show fractional crystallization trends from dunites through clinopyroxene peridotite and pyroxenite, to gabbros. There are systematic trends among the primary oxides, e.g., CaO, TiO_2, and Al_2O_3, with MgO, suggesting a fractional crystallization trend. SiO_2 and Al_2O_3 increased, which coupled with decreasing MgO, suggested olivine fractionation. The negative correlations of CaO and Al_2O_3 with MgO meant the accumulation of spinel and mafic minerals. The compositions of olivines from the dunite and clinopyroxene peridotite in the Hongshishan plot within the Alaskan Global trend fields displayed a typical fractional crystallization trend similar to olivines in an Alaskan-type complex. The clinopyroxenes in the clinopyroxene peridotite primarily occur as a diopside and appear in the field of an Alaskan-type complex. The absence of orthopyroxene, less hydrous, and free of fluid inclusions in the chrome spinels means the absence of a magmatic origin of chromite-bearing peridotites in hydrous parental melts or scarce hydrous melts. Serpentinization, carbonatization, subduction modification, and enrichment may account for the LILE-enrichment and HFSE-depletion of peridotite rocks. Negative Eu anomalies and REE fractionations of mafic-ultramafic rocks may not be directly attributed to crustal assimilation. Petrological, mineralogical, and geochemical characteristics indicated the Hongshishan complex is not the member compositions of a typical ophiolite. However, it displays many similarities to Alaskan-type mafic-ultramafic

intrusions related to subduction or arc magmas setting at ~366.1 Ma and suffered subduction modification and enrichment. The Hongshishan complex is a unique Ir-Ru-rich chromite deposit in the southern margin of the Altaids orogenic belt. Chromites occur primarily in light yellow dunites, with banded, lenticular, veined, thin-bedded, and brecciated textures. Part of the chromite enrichment in IPGE (Os, Ir, Ru) and the chondrite-normalized spider diagram of PGE showed steep right-facing sloped patterns similar to those of the PGE-rich ophiolitic chromites.

Keywords: Beishan orogenic collage, Hongshishan ophiolite, Alaskan-type complex, petrology, fractional crystallization, chromite and PGE mineralization, subduction tectonic environments

INTRODUCTION

Generally, Alaskan-type complexes show the following characteristics: they are related to the subduction environment and composed of a central dunite body grades outward into wehrlite, clinopyroxenite and gabbroic lithologies, occasionally occurring olivine clinopyroxenite, hornblendite clinopyroxenite, hornblendite, and hornblendite gabbro, characterized by the dominance of olivine, clinopyroxene, hornblende and the absence of orthopyroxene and plagioclase. Pyroxenes in the complexes are almost exclusively clinopyroxenes (mainly diopside in composition) and olivines are occasionally Mg-rich (Irvine 1967; Himmelberg and Loney 1995; Krause et al., 2007; Su et al., 2012, 2014; Habtoor et al., 2016). Magma composition comes from the mantle with no significant crustal contamination (Helmy and El Mahallawi, 2003; Tian et al., 2011). Geochemically, the complex shows a slight LREE enrichment and weak or no Eu anomalies, an elevated LILE, and obvious low high-field strength elements (HFSE) such as Nb, Ta, and Ti (Himmelberg and Loney, 1995; Helmy and El Mahallawi, 2003; Pettigrew and Hattori 2006; Ripley 2009).

Various hypotheses have been suggested to describe the petrogenesis of Alaskan-type complexes such as fractional melting in the mantle (Irvine, 1967; Taylor, 1967), fractional crystallization from magma mixtures (Sha, 1995; Farahat and Helmy, 2006; Habtoor et al., 2016), fractional crystallization from a common hydrous parental magma without significant crustal contamination (Farahat and Helmy, 2006; Tian et al., 2011), depleted mantle metasomatized by subduction-related melts/fluids (Su et al., 2014), and tectonic emplacement of fragments of a pre-existing body (Efimov, 1998). These hypotheses have generated some controversy and contradictions. For example, for fractional melting, Taylor (1967) and Irvine (1967) suggested that petrologic and mineralogical relationships among ultramafic rocks can be interpreted by multiple magmatic intrusion mechanisms; however, this mechanism runs contrary to the diagenetic order of most Alaskan-type complexes. The viewpoint of depleted mantle metasomatized by subduction-related melts/fluids favors multiple magmatic pulses instead of fractional crystallization within a common parental magma (Su et al., 2014).

Alaskan-type complexes generally form in arc-related tectonic environments (Taylor 1967; Irvine, 1974; Helmy and El Mahallawi, 2003; DeBari and Coleman 1989; Brugmann et al., 1997; Helmy et al., 2014; Saleeby 1992; Foley et al., 1997; Valli et al., 2004; Su et al., 2012, 2014) or at the change from the arc setting to the extensional regime (Tistl et al., 1994; Mues-Schumacher et al., 1996; Chen et al., 2009; Tian et al., 2011; Spandler and Pirard, 2013; Helmy et al., 2015). According to Tistl (Tistl et al., 1994) and Mues-Schumacher (Mues-Schumacher et al., 1996), Alaskan-type intrusions also represent geodynamic setting variations from arc-related convergent systems to a local extension, e.g., reararc–backarc setting or strike-slip system (Spandler and Pirard, 2013; Helmy et al., 2015). However, Alaskan-type candidate complexes formed during an extensional setting are rare and the characteristics of the complexes differ significantly from typical ones, and even some ultramafic rocks, generated during post-collision extension or an intracontinental rift stage, do not belong to Alaskan-type complexes (Su et al., 2013). Alaskan-type complexes are considered as possible mantle plume-related intrusions (Ishiwatari and Ichiyama, 2004; Pirajno, 2004; Farahat and Helmy, 2006). In this hypothesis, plume interaction may account for the superheating required to generate an Alaskan-type intrusion, and similarities with Alaskan-type intrusions are nothing but trace element geochemistry (Farahat and Helmy, 2006). Moreover, the mafic rocks associated with a plume do not possess Alaskan-type intrusion characteristics (Pirajno, 2004).

Based on the above disputes, determining the nature of the mafic-ultramafic intrusions and their tectonic setting is significant to understand the tectonic evolution of the orogenic belts (Helmy and Mogessie, 2001; Helmy, 2004, Helmy, 2005; Su et al., 2012, 2014; Deng et al., 2015a,b; Khedr et al., 2020; Wang et al., 2021). Significantly, chromite mineralization associated with a typical Alaskan-type complex (Garuti et al., 2002, 2003; Krause et al., 2007; Khedr et al., 2020; Wang et al., 2021) and the Gaositai complex in North China Craton (Zhou and Bai, 1992; Chen et al., 2009; Tian et al., 2011) is found in the core of concentrically zoned intrusions. In contrast with high-Al and high-Cr chromites in ophiolites, chromites formed in Alaskan-type complexes are characterized by high Ti, high oxygen fugacity (fO_2), and Fe^{3+} enrichment; furthermore, their sub-economic PGE mineralization draws the attention of geologists (Zhou and Bai, 1992; Tian et al., 2011; Khedr et al., 2020).

The Hongshishan mafic-ultramafic rocks were previously considered as component parts of an ophiolitic mélange and occur as a suture in the plate of Kazakhstanian-Junggar and

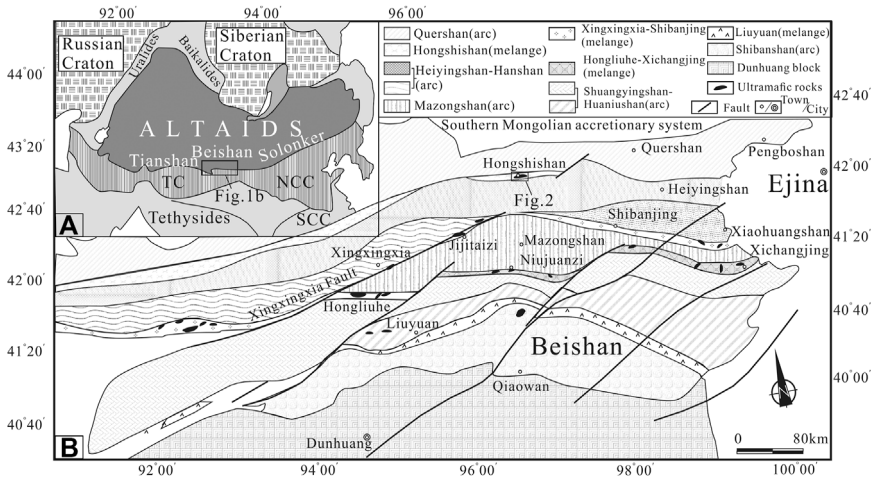

FIGURE 1 | (A) Simplified tectonic sketch map of Asia showing the location of the Beishan orogenic collage. **(B)** Simplified tectonic map of the Beishan orogen showing the tectonic subdivisions and study area (modified after Xiao et al., 2010; Song et al., 2015). TC, Tarim Craton; NCC, North China Craton; SCC, South China Craton.

Siberian (Gong et al., 2003; Huang and Jin, 2006a; Xiao et al., 2010), but absent in the corresponding mantle peridotites and cumulates and contain banded chromites in core dunites from the concentrically zoned complex (Wei, 1978; Yang et al., 2010; Wang et al., 2013; Peng et al., 2016). The Hongshishan complex differs from the SSZ ophiolite but shares many similarities with a Dahanib Alaskan-type complex in the Southern Eastern Desert of Egypt (Khedr and Arai, 2016; Khedr et al., 2020), the Uralian-Alaskan-type complex (Garuti et al., 2002, 2003; Krause et al., 2007), and a series of complexes in Beishan Terrane and Middle Tianshan Terrane (Su et al., 2012, 2013, 2014). But the emplacement mechanism, geochemical composition, and evolution of the Hongshishan complex, especially chromite origins, are poorly understood.

Although much work has been conducted on chronological and geochemical studies of the Hongshishan mafic-ultramafic complex (Wei et al., 2004; Huang and Jin, 2006b; Wang et al., 2014; Shi et al., 2017), very little research has provided evidence for Alaskan-type complexes, thought to have formed above subduction zones, and no attention has been paid to the inherent formation of chromites related to an Alaskan-type complex and may shed light on its metallogenic significance (Khedr and Arai, 2016; Khedr et al., 2020).

In this study, we present new zircon U–Pb isotopic data, silicate chemical compositions, chromian minerals of spinels, olivines, and clinopyroxenes, which should provide new insights and realizations regarding tectonic evolution in the Beishan orogenic collage.

GEOLOGICAL SETTING

The Beishan orogenic collage, between the Kazakhstanian-Junggar plate to the north and the Tarim-North China craton to the south, is framed by the southern Mongolia accretionary system in the north and the Dunhang block in the south (**Figure 1**) (Xiao et al., 2010; Song et al., 2015). It marks the attachment to the Eastern Tianshan orogenic belt by the Xingxingxia ductile left-lateral strike-slip fault, though it is not well defined and covered by the Badain Jaran Desert to the east despite occasional ophiolites (Zuo et al., 1991; Liu and Wang, 1995; Xiao et al., 2010). The development of the Beishan orogenic collage assists the final attachment of the Tarim-North China plate to the southern accretionary orogenic belt of the southern Altaids (Ao et al., 2010; Guo et al., 2012; Mao et al., 2012).

Spatially, the Beishan orogenic collage consists of several tectonic units formed by multiple accretionary orogenies, from north to south, Hongshishan mélange, together with the Shibanjing-Xiaohuangshan, Hongliuhe-Yushishan-Niujuanzi-Xichangjing, and Liuyuan ophiolitic mélange, separate the Beishan orogenic collage into several discrete terranes units, Queershan, Hanshan, Mazongshan, Shuangyingshan and Shibanshan terranes (**Figure 1B**).

At the end of the Early Paleozoic, the Hongliuhe-Niujuanzi-Xichangjing ocean closed, followed by attachment and soft collision during the Devonian between the diverse accreted tectonic units formed in the margin of Kazakhstan and the Tarim plate including magmatic arcs, accretionary complexes etc., and formed a uniform continent (He et al., 2005; Song and Pirard., 2013, 2015). During the Early Carboniferous, continental cracking and intense stretching occurred in the Heiyingshan area between the Quershan and the Gongpoquanarc-accretionary system, forming a rift basin along Kangguer, Hongshishan, and Pengboshan (He et al., 2005; Xia et al., 2005; Yang et al., 2010; Peng et al., 2016). The amalgamation and accretion of the above tectonic units gave rise to strong Late Permian to Triassic deformations that included thrust imbrication and strike-slip faulting (Xiao et al., 2010).

Among the mélanges mentioned above, the so-called Hongshishan ophiolitic mélanges lie in the northern part of the orogenic collage and occupy an important position as the

distribution center for the biogeography of Carboniferous North China and South China. Angara floras were distributed north of the Hongshishan suture and Carboniferous marine fauna, the Cathaysia floras were only distributed south of the Duhuang block (Yue et al., 2001), whereas Hongshishan contained no complete ophiolite stratigraphy (Peng et al., 2016; Shi et al., 2018).

Gabbros in Hongshishan used LA-ICP-MS and SHRIMP U-Pb to generate $^{206}Pb/^{238}U$ weighted mean ages of 346.6 ± 2.8 and 357 ± 4 Ma respectively (Wang et al., 2014; Shi et al., 2017). The fossils *Leiotrites netiux H aequ Punctatiporites planus H aequ* that occurred in the volcanic-sedimentary rocks that covered the ophiolite suggested the Hongshishan mélange formed during the Early Carboniferous (Wei, 2004). Previous geochemical and Sm/Nd isotope characters indicated that the Hongshishan basic volcanic rocks formed in a MORB tectonic environment (Huang and Jin, 2006a; Wang et al., 2014) and the Hongshishan complex was thought to form during the Carboniferous-Permian and suffered at least three stage structural deformation metamorphisms before returning to terrene by shearing at the Late Permian (Wei et al., 2004; Huang and Jin, 2006b). The thrusts and imbricate structures that occurred in the north and south margins of Hongshishan mélanges indicated a southward translation (Xiao et al., 2010).

GEOLOGICAL AND PETROGRAPHY CHARACTERS OF COMPLEX ROCKS

The fish-shaped Hongshishan complex situated in the north of the Beishan orogenic collage strikes E-W, approximately 7 km long and up to 2 km wide (**Figure 2**). The melange contains Carboniferous marine sandstone, sandy slate, chert, chlorite schist, and ultramafic-mafic rocks. The ultramafic and mafic complex intrude in the Carboniferous metamorphic volcanic–sedimentary sequences (Zuo et al., 1990a; Zuo et al., 1990b; Zuo et al., 1991). The complex comprises east and west segments. The west segment constitutes the main structure of the complex, dominated by clinopyroxene peridotite and dunite in the core, with accompanying mafic intrusions that include pyroxenite, gabbro distributed in the ultramafic and mafic rocks as lenticular, banding, and isolated. Grading outward into clinopyroxene peridotite with numerous dunite schlierents in the North-West part. Altered gabbro, pyroxenite, and basaltic schist sit along the north and south rims. The ultramafic and mafic complex inclines steeply or suberect in the south and dips northward in the north margin. The Hongshishan complex contains no harzburgites.

The surrounding stratigraphy of the complex consists of the Lower Carboniferous Lvtiaoshan Formation in the north and the Baishan Formation in the south. The former, formed in a calc-alkaline volcanic environment, consists of sandy slate, metasandstone, quartz sandstone with siliceous rocks, basalt, andesite as intercalated beds and gives rise to a chlorite sericite quartz schist, tuffaceous metasandstone, fused breccia, andesite, and rhyolite (Huang and Jin., 2006c; Peng et al., 2016). Even largely intruded by Permian biotite monzogranite, intermediate-basic dykes and covered by Quaternary sediments in the middle segment, the complex outlines a concentrically zoned structure and resembles Alaskan-type complexes (Taylor, 1967; Himmelberg and Loney, 1995; Garuti et al., 2002, 2003; Krause et al., 2007; Tian et al., 2011; Khedr et al., 2020).

Dunite

The dunites are situated along the south and north-western margins, in the central part and occasionally scattered as schlieren in the clinopyroxene peridotite of the western border and are divided into two types: light yellow dunites and yellow-green dunites (**Figure 2**). The light yellow dunites underwent silicification and carbonatation, were exposed to the surface and their color lightened (**Figures 3A,D,E**; **Figures 4A–K**). In the outcrop, dunites show small-scale layering features and typical cumulate textures (**Figure 3F**). These rocks primarily consist of olivine pseudomorphs and chromites with minor altered clinopyroxene relics (<5 vol%) and magnitites. Olivines in light yellow dunite are nearly all altered to antigorite-lizardite-magnetite assemblages exposing mesh textures due to serpentinization. The light yellow dunites comprise most of the chromite orebodies (**Figures 4A–G**).

Despite undergoing serpentinization, yellow-green dunites with unaltered olivine cores or whole grains are relatively fresh compared to light yellow dunites. Olivines in yellow-green dunites are homogenous, fresh, and free of opaque inclusions, and show crystalized textures of variable size, subeuhedral-euhedral crystals, and angular shapes with variable grain sizes (from 0.3 to 0.8 mm; **Figures 5A,B**). Dunites are composed of cumulus olivines with varying densities, disseminated chromian spinels, and subordinate Cpxs (<3 vol%). Serpentinite and carbonatite veins cut through a large number of olivine grains. Dunite schlierents in clinopyroxene peridotites are the exclusive metallogenic rocks of chromites. Chromian spinels in yellow-green dunite are generally sparsely disseminated or scattered texture (**Figures 5J,L**).

Clinopyroxene Peridotite

Clinopyroxene peridotites are widely exposed in the central and east areas and weathered red with nodular appearances (**Figures 3G,H**). In the southeast of the biotite monzogranite, clinopyroxene peridotites underwent serpentinization, carbonatization, silicification, and turned brown due to abundant iron oxide. The boundary between clinopyroxene peridotites and dunites normally curves and transitions gradually into clinopyroxene dunites. Occasionally, clinopyroxene peridotites alternate with dunite and pyroxenite layers and cut by dunite veins (**Figure 3D**), indicative of magma differentiation and evolution. Clinopyroxene peridotites consist of olivines, clinopyroxenes, amphiboles, and some altered minerals with olivines (80–85 vol%), Cpxs (5–10 vol%), Cr-spinels (<3 vol%), and opaques (<2 vol%). Olivines are subeuhedral columnar crystals that primarily morph into serpentines. Clinopyroxenes are mainly diopsides and sometimes replaced by neogenic pargasites, edenites, and actinolites at their edges (**Figures 5C,G,I**). Due to serpentinization and weathering, clinopyroxenes were oriented

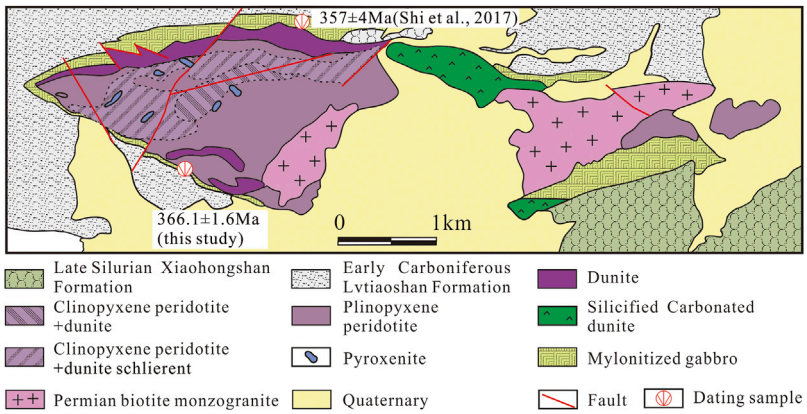

FIGURE 2 | Simplified geological map of the Hongshishan complex (modified after Wei, 1978).

as pseudomorphs in the olivine matrix and were mostly substituted by serpentines, carbonate minerals, tremolites, and magnetites.

Gabbro

Gabbros are exposed on the north and southeast margins of the mafic-ultramafic complex (**Figure 2**). They have equigranular texture and are composed of clinopyroxenes (40–45 vol%), plagioclases (35–45 vol%), hornblendes (<5 vol%), and 3–5% opaque minerals (mostly magnetite). Several outcrops in the field show signs of rhythmic layering of clinopyroxenes and plagioclases (**Figures 3B,C**). Most clinopyroxenes morph into actinolites or tremolites, and plagioclases normally change into zoisites (**Figures 5D,F,H**). Gabbros on the north and southeast margins often show strong foliation with mylonitic textures and sharp tectonic contacts to the peridotites. S-C fabrics and rotational speckles characterize the dextral ductility shear (Huang and Jin, 2006b). Additionally, as a general feature of Alaskan-type complexes, several gabbroic dykes with magmatic layering intrude into dunites and clinopyroxene peridotites (**Figure 3C**). The dykes may form in later-stage residual melts after fractionation rather than the cumulate in ophiolite (Irvine, 1974; Snoke et al., 1981; Himmelberg and Loney, 1995). Unaltered gabbro samples from the southern margin were collected for zircon U–Pb dating and geochemistry analyses.

Chromite

Chromites occur primarily in light yellow dunites, with subordinate Cpx-enriched dunites. Classified by shapes and spatial distributions of the chromite orebodies, the orebodies are labeled as: banded, lenticular, veined, thin-bedded, and brecciated texture (**Figures 4A–G**). Nearly 70–80% of modal chromites in Hongshishan show primary magmatic layering where individual seams involve layers of massive, spotted, schlieren, and banded-texture chromites. Banded chromites, occasionally with crossbedding, are primarily composed of massive and varying degrees of disseminated chromian-spinel grains that interbed alternately with inch-scale thickness of layers chromian spinels (**Figures 4F,H–L**). Orebodies of the banded subzone are tabular and more extensive laterally. Many bands show small-scale faulting and cataclasis.

Most chromites show weak deformations with polygonal or angular crystal appearances and pull-apart fractures, cataclastic textures (**Figure 4D**), and occasional ductile deformations (such as elongated worm-like shapes), and cluster to form chromite bands or disseminated varieties, though morphologically distinct from podiform chromites in supra subduction zone environments (Zhou et al., 2014). Skeletal textures also occurred in chromites and were interpreted as indicators for rapid crystallization, possibly due to supersaturation processes (Greenbaum, 1977). The chromite textures in Hongshishan showed that disseminated chromites crystallized earlier than the massive chromites.

SAMPLES AND ANALYTICAL TECHNIQUES

Representative samples from the Hongshishan mafic-ultramafic complex, including dunite, clinopyroxene peridotite, pyroxenite, and gabbro came from the western and eastern part of the intrusion. Samples for LA-ICP-MS U–Pb dating were collected from gabbros in the southern margin of the complex. Polished thin sections made from unaltered ultramafic-mafic rocks and chromites ore samples were chosen and analyzed by electron microscopy.

Major, Trace, and Rare-earth Elements

The determination of major, trace, and rare-earth elements was conducted at the Beijing GeoAnalysis Technology Co., Ltd. using X-ray fluorescence (XRF-1800; SHIMADZU) on fused glasses. Inductively coupled plasma mass spectrometry (ICP-MS, 7500; Agilent) was conducted at Beijing Createch Testing Technology Co., Ltd. on samples after acid digestion in Teflon bombs. Loss on ignition was measured after heating to 1,000°C for 3 h in a muffle furnace. The precision of the XRF analyses was within ±2% for oxides with >0.5 wt% and within ±5% for oxides >0.1 wt%. Sample powders (~40 mg) were placed in Teflon bombs and dissolved using a mixture of HF and HNO_3 for 48 h at 190°C. The solution

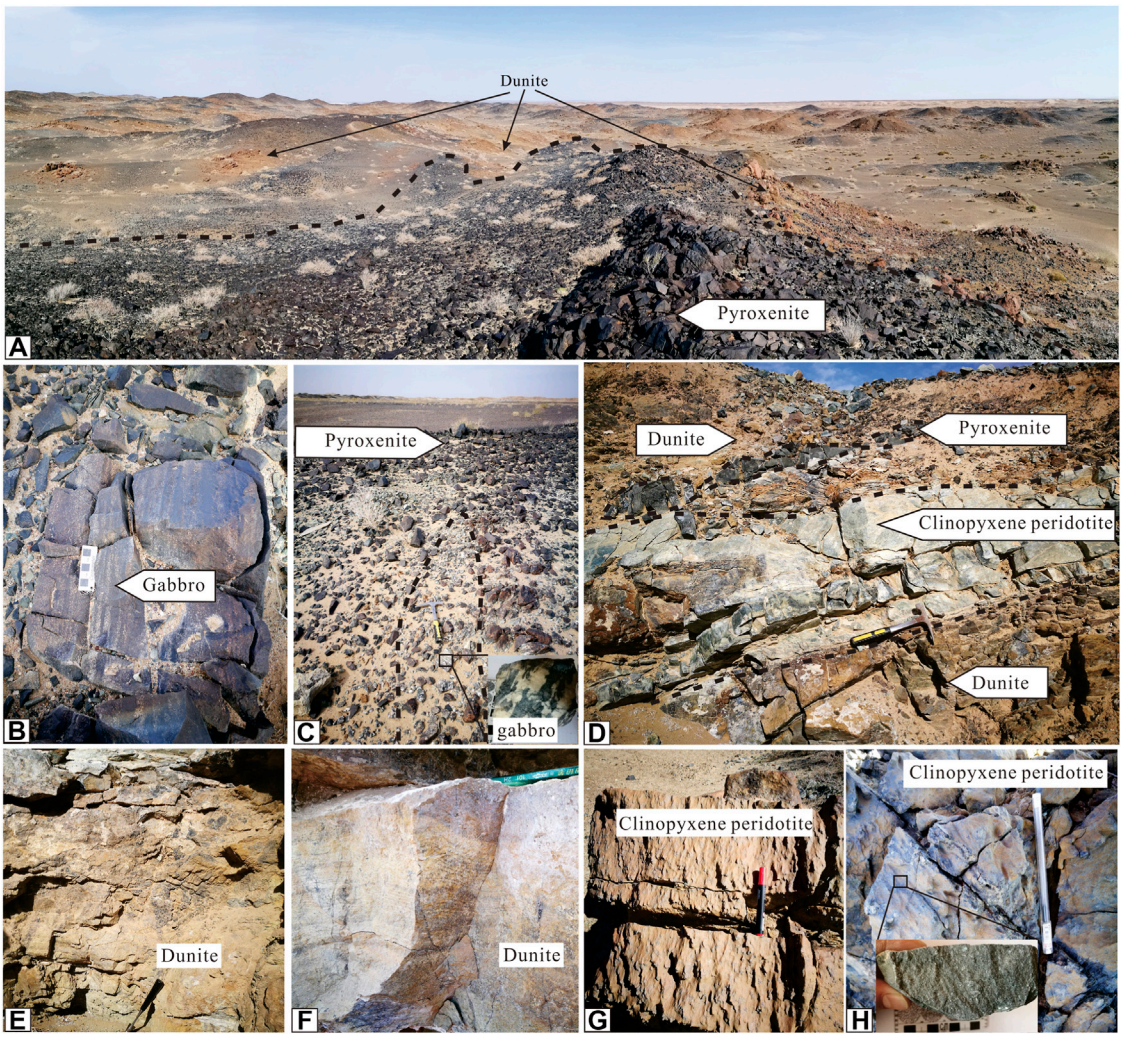

FIGURE 3 | Field photographs of Hongshishan ultramafic–mafic complex. **(A)** Dunites are intruded by pyroxenite; **(B)** Gabbro with the rhythmic layering of clinopyroxene and plagioclase, showing the magmatic fractional crystallization; **(C)** Coarse grain gabbro dyke intruded into pyroxenite; **(D)** Dunite layers alternating with clinopyroxene peridotite, pyroxenite layer; **(E)** The light yellow dunites contain chromites; **(F)** Dunite showing typical cumulate textures and small-scale layering features (0.2–0.6 cm); **(G, H)** Clinopyroxene peridotites were weathered red with nodular appearances.

was evaporated to dryness, re-dissolved using concentrated HNO_3, and evaporated at 150°C to dispel any fluorides. Samples were diluted to approximately 80 g for analysis after dissolution in 30% HNO_3 overnight. An internal standard solution containing Rh was used to monitor signal drift during the analyses. Results from USGS standards indicated the uncertainty for most elements was ±5%.

Mineral Chemistry

The chemistry of unaltered minerals (olivines, pyroxenes, and chrome spinel, etc.) in silicates and oxides was conducted by wavelength-dispersive X-ray analysis using a JEOL electron-probe micro analyzer (EPMA) JXA-8230 at the Institute of Mineral Resources, Chinese Academy of Geological Sciences. We used 15 kV for the acceleration voltage, 20 nA for the beam current, a 5 μm beam diameter, and the counting time was between 20 and 40 s for major elements and 40–60 s for minor elements. SPI mineral standards (USA) were used for calibration. The precision for all elements analyzed exceeded 98.5%. The Cr- and Mg-numbers (Cr# and Mg#) of the chromian spinel were the Cr/(Cr + Al) and Mg/(Mg + Fe^{2+}) atomic ratios, respectively. We assumed all Fe in silicates was ferrous.

Geochronology

Zircon U-Pb dating was conducted using an LA-ICPMS at Beijing GeoAnalysis Co., Ltd. The Resolution SE model laser ablation system (Applied Spectra, United States) was equipped with an ATL (ATLEX 300) excimer laser and a Two-Volume S155 ablation cell. The laser ablation system was coupled to an Agilent 7900 ICPMS (Agilent, United States). Zircons were mounted in epoxy discs, polished to expose the grains, ultrasonically cleaned in ultrapure water, then cleaned again prior to the analysis using AR grade methanol. Pre-ablation was conducted for each spot analysis using five laser shots (~0.3 μm in depth) to remove potential surface contamination. The

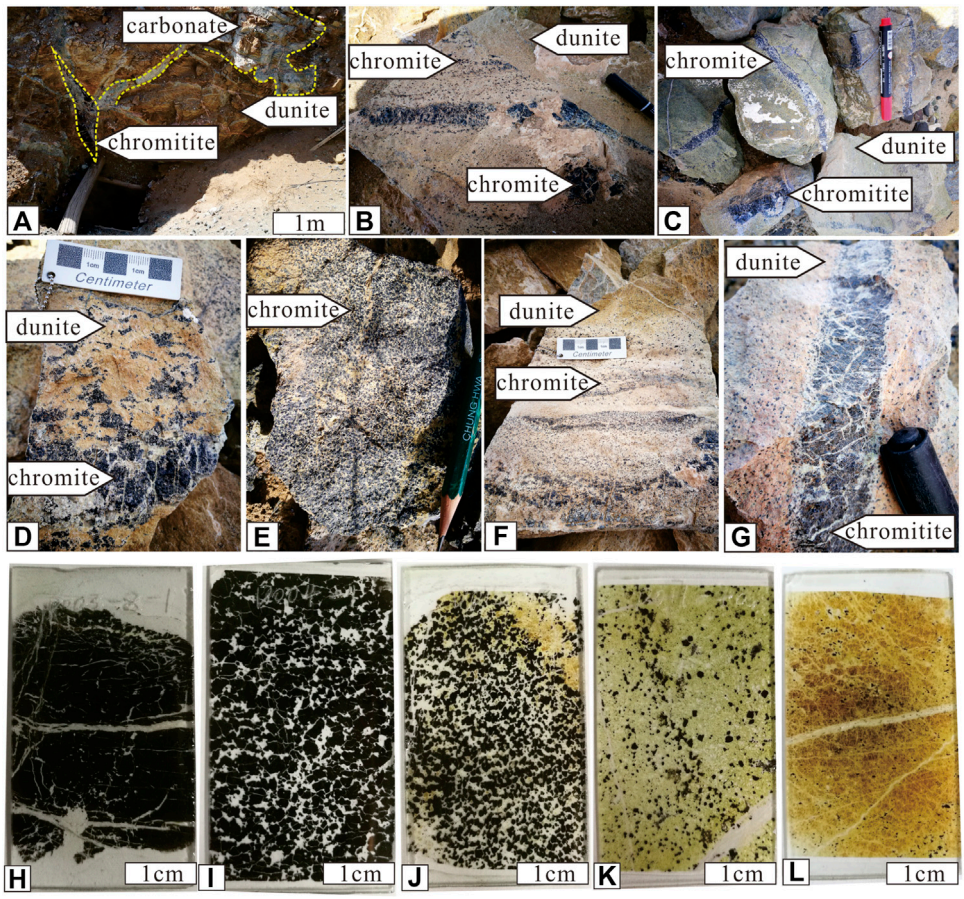

FIGURE 4 | Field and sample photographs of peridotite-hosted chromites in the Hongshishan complex. **(A)** Lenticular chromite orebody in carbonated dunite; **(B)** Banded chromite orebody cut by dunite; **(C)** Veined chromite orebodies in dunite; **(D)** Brecciated chromites; **(E)** Dense disseminated chromites; **(F)** Banded chromite composed of medium density disseminated, sparsely disseminated, and brecciated chromites; **(G)** Veined chromite crosscutting dunite with sparsely disseminated chromites; **(H)** Massive chromites; **(I)** Dense disseminated chromites; **(J)** Medium density disseminated chromites; **(K)** Sparsely disseminated chromites; **(L)** Scattered chromites. (**H–L**: thin-section).

analysis was performed using a 30 μm diameter spot at 5 Hz and a fluence of 2 J/cm^2.

Zircon 91500 and GJ-1 were used as primary and secondary reference materials, respectively. Zircon 91500 was analyzed twice and GJ-1 was analyzed once every 10–12 analyses. Typically, 35–40 s of the sample signals were acquired after 20 s of gas background measurement. NIST 610 and ^{91}Zr were used to calibrate the trace element concentrations as the external reference material and the internal standard element, respectively. The ages of the reference materials in the batch are as follows: 91,500 (1061.5 ± 3.2 Ma, 2σ), GJ-1 (604 ± 6 Ma, 2σ), and agreed with the reference value within definite uncertainty.

RESULTS

Major, Trace, and REE Silicate Geochemical Compositions

Supplement 1 lists the analytical data of major, trace, and REE for samples from each rock unit of the Hongshishan complex. Disseminated chromian spinels-bearing dunites had high volatile levels (LOI. 9.43–14.83 wt%, except for D002-7 and D003-6). For the dunites, SiO_2 compositions varied from 35.23 to 38.82 wt%, Al_2O_3 from 0.39 to 4.45 wt%, and TiO_2 from 0.00 to 0.07 wt%. While the composition of clinopyroxene peridotites was SiO_2, 29.55–42.61 wt%, Al_2O_3, 0.43–7.97 wt%, TiO_2, 0.00–0.11 wt%, they were nevertheless distinguished from the dunites by much higher Ca concentrations (CaO 1.13–8.68%). Pyroxenite components had the following compositions, SiO_2 from 40.65 to 45.76 wt%, Al_2O_3 from 9.31 to 16.05 wt%, and TiO_2 from 0.07 to 0.14 wt%; gabbros SiO_2 from 42.01 to 49.58 wt%, Al_2O_3 from 12.81 to 22.25 wt% and TiO_2 from 0.02 to 0.30 wt%. These compositions reflect depleted mantle melts as the primary intrusion source.

MgO compositions decreased systematically from the dunites (23.53–43.02 wt%) and clinopyroxene peridotites (29.43–36.23 wt%), followed by pyroxenites (14.75–31.85 wt%) and gabbros (8.46–18.22 wt%). In Harker diagrams (**Figure 6**), these major compositions, e. g. Al_2O_3, CaO, and TiO_2 were lowest in dunites and peridotites cores, increased gradually in pyroxenite and maximized in the marginal gabbros. Most dunites have low

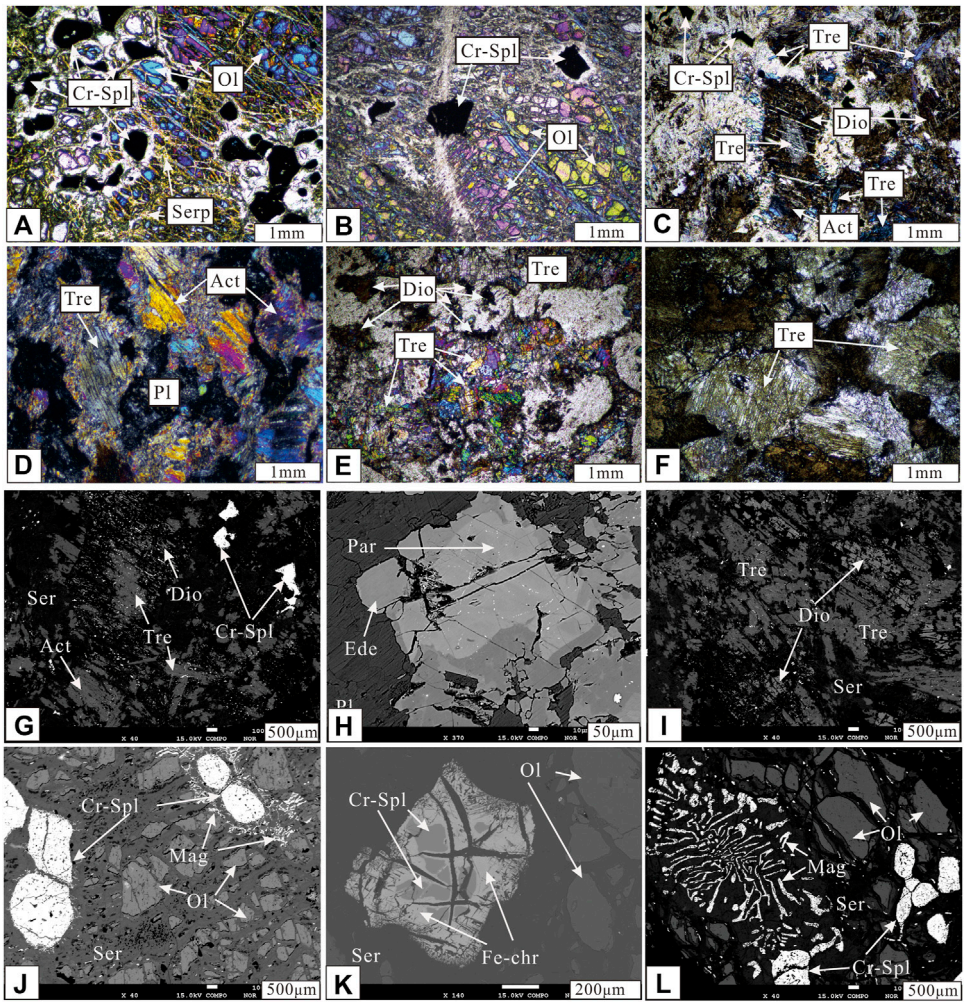

FIGURE 5 | Photomicrographs and backscattered electron (BSE) images of clinopyroxene peridotite and dunite. **(A)** Medium-density disseminated chromites in dunites; **(B)** Scattered chromites in dunites; **(C)** Diopsides in clinopyroxene peridotite are replaced by neogenic tremolite and actinolite; **(D, F)** Diopsides in altered gabbros are altered to actinolite and tremolite, and plagioclases are commonly altered to zoisite; **(E)** Residual diopsides in serpentine and neogenic tremolite; **(G, I)** Neogenic actinolite and tremolite in clinopyroxene peridotite; **(H)** unaltered pargasite and endenite in altered gabbro; **(K)** Chrome spinel (dark gray) with melting corrosion structure, altered to ferritchromite (Fe-chr) (lighter gray) along cracks and margins of Cr-spinel in scattered chromites-bearing dunite; **(J, L)** Medium density disseminated subhedral chromites and skeleton-texture magnetite in dunite. (**A–E**: cross-polarized light; **F**: plane-polarized light; **G–L**: backscattered electron (BSE) images; Ser—serpentine; Act—actinolite; Dio—diopside; Tre—tremolite; Par—pargasite; Ede—endenite; Ol—olivine; Cr-Spl—chrome spinel; Mag—magnetite; Pl—plagioclase; Fe-chr—ferritchromite).

CaO levels (<1 wt%), whereas clinopyroxene peridotites and pyroxenites had higher CaO concentrations (1.13–8.68 wt% and 4.23–12.21 wt%, respectively). The gabbros had the highest CaO concentrations (10.66–15.06 wt%). TiO_2 levels in the dunites were virtually non-existent, but increased in clinopyroxene peridotites (0.00–0.11 wt%) and pyroxenites (0.07–0.14 wt%), and reached a maximum in the gabbros (0.02–0.30 wt%). The average Mg# (Mg/(Mg + Fe) atomic ratio) accordingly decreased from 0.90 in dunites, 0.90 in clinopyroxene peridotites, followed by 0.87 in pyroxenites to 0.82 in the marginal gabbros (**Supplementary Table S1**).

In terms of trace elements, dunites contain enriched levels of large-ion lithophile elements (LILE) (like Cs), high field strength elements (HFSE) (U, Zr, Hf), and Er. Also, significantly negative anomalies in Nb, Ba were observed, and Ti to a lesser extent (Nb/La ratios from 0.12 to 0.19, Th/Yb ratios from 0.39 to 2.78, Ta/La from 0.03 to 0.18 and Nb/Th from 0.01 to 0.55; Supplement 1). The gabbroic rocks shared many geochemical similarities with pyroxenites. They had higher trace element abundances and distinctive Ba, Pb, Cs, and Ti anomalies than the ultramafic rocks, which had lower Rb and Ba levels (**Figure 7**).

Different from the dunites in the Alaskan complex with identical flat REE patterns (Su et al., 2014; Habtoor et al., 2016), the dunites in Hongshishan display higher REE abundances (average 6.04 ppm) and enriched light REE (LREE) values relative to heavy REE (HREE) with high La_N/

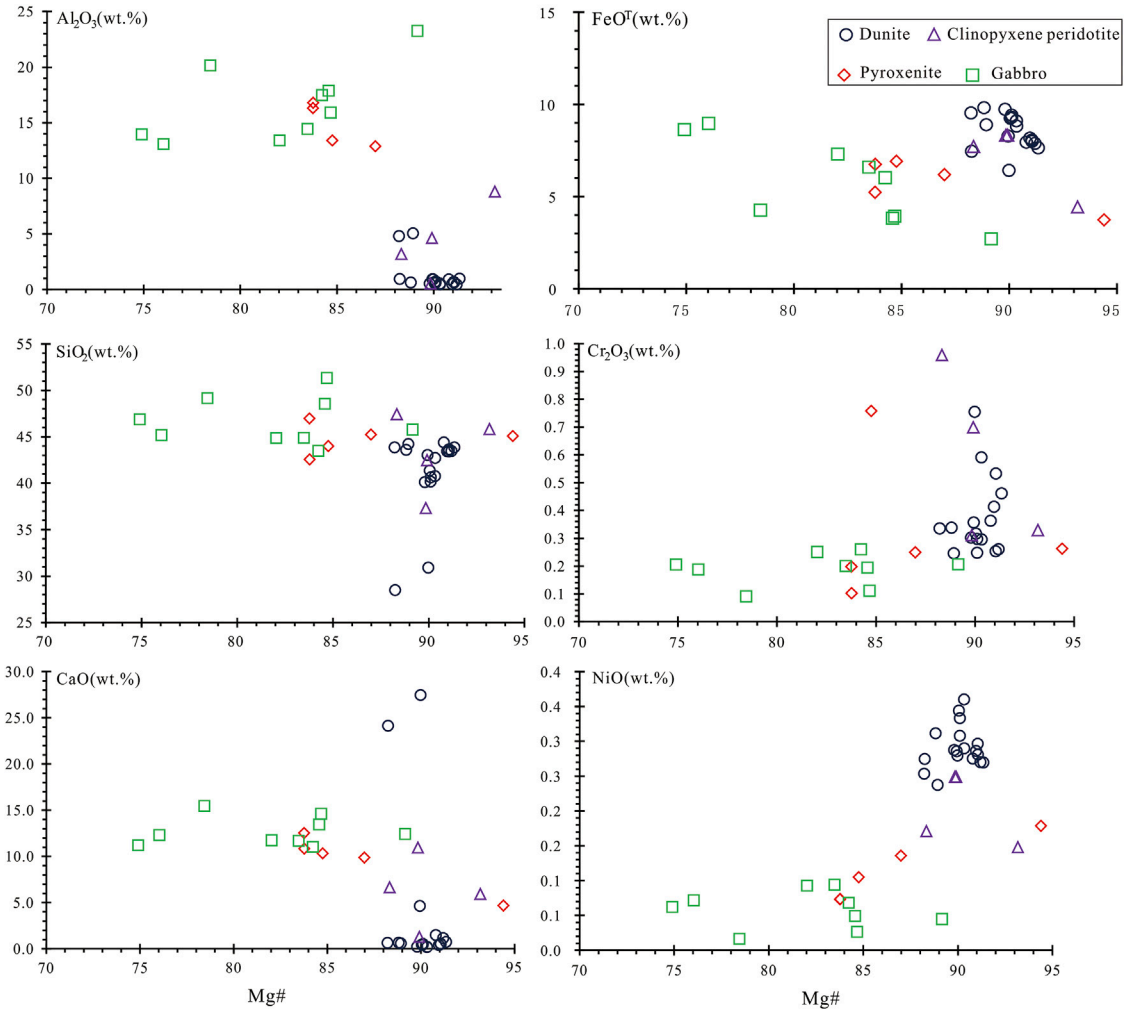

FIGURE 6 | Hark diagrams of oxides (Al_2O_3, FeO_T, SiO_2, Cr_2O_3, CaO, and NiO) vs. Mg# of the bulk-rock in the Hongshishan complex.

Yb_N ratios (average 4.49; **Supplementary Table S1**), negative Eu anomalies and pronounced positive Er anomalies with a typical V (or U)-shaped pattern (Song and Frey, 1989; Wang et al., 1996). The clinopyroxene peridotites showed negative Eu anomalies and wide compositional HREE variations. Pyroxenites and gabbros showed nearly flat REE patterns and positive Eu, Er anomalies (**Figure 7**). The positive Eu anomalies in the pyroxenites and gabbros indicated the presence of plagioclase in the crystallized rocks, which was in accord with other petrographic investigations. The positive Sr anomalies were consistent with the positive Eu anomalies and implied plagioclase accumulation.

Zircon U–Pb Ages

One gabbro sample collected from the south margin of the mafic-ultramafic complex was selected for zircon U–Pb dating. Zircons separated from the sample ranged from 30 to 100 μm and were generally euhedral, colorless, and transparent. The cathodoluminescence (CL) images with internal growth zoning indicated a magmatic crystallization origin. (**Figure 8**). Sixteen-grain effective data formed a concordant group in the Concordia diagram with a weighted mean age of 366.1 ± 1.6 Ma (MSWD = 1.17), the age reflects the gabbro emplacement time. This age predates previous gabbro geochronological data and is regarded as an estimate of the Hongshishan complex crystallization age. Supplement 2 gives the analytical data of the Hongshishan gabbro Zircon U-Pb age.

Mineral Chemistry of Chromian Spinels, Olivines, and Clinopyroxenes

The microprobe analysis data for chromian spinels, olivines, clinopyroxenes, hornblendes in the Hongshishan mafic-ultramafic complex are listed in **Supplementary Table S3**.

Chromian spinels in veins and massive chromites have average Al_2O_3 wt% levels of 0.97–25.81 (average 16.6 wt%), Cr_2O_3 (40.52–58.23, average 48.8), Fe_2O_3 (0–2.4, average 4.2), FeO

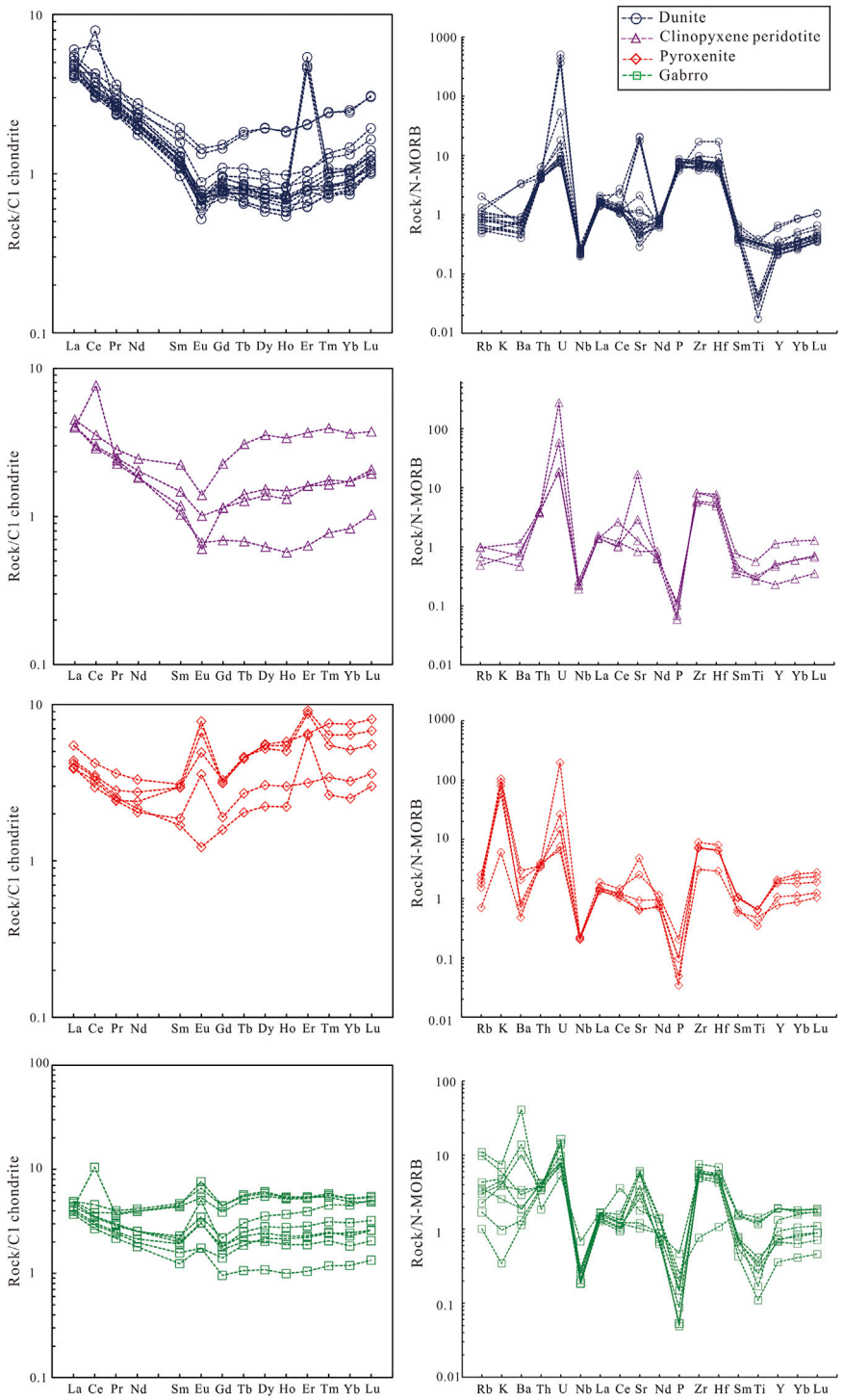

FIGURE 7 | N-MORB normalized spider diagrams and C1 chondrite-normalized REE patterns of the Hongshishan complex. C1 chondrite-normalizing values are from Sun and McDonough (Sun et al., 1989), primitive mantle-normalizing values are from McDonougha and Sun (McDonough and Sun., 1995).

(12.97–29.15, average 19.3), TiO_2 (0.06–0.46, average 0.2) and MgO (2.24–14.73, average 9.8), with narrow Cr# ranges (from 0.52 to 1.00; 0.70 on average) and Mg# (0–0.63; 0.38 on average). Various density degrees of chromian spinels in dunites have wide oxide ranges with Al_2O_3 ranging from 0 to 29.27 wt% (average 10.07 wt%), Cr_2O_3 from 0.20 to 57.74 (average 36.63 wt%), Fe_2O_3

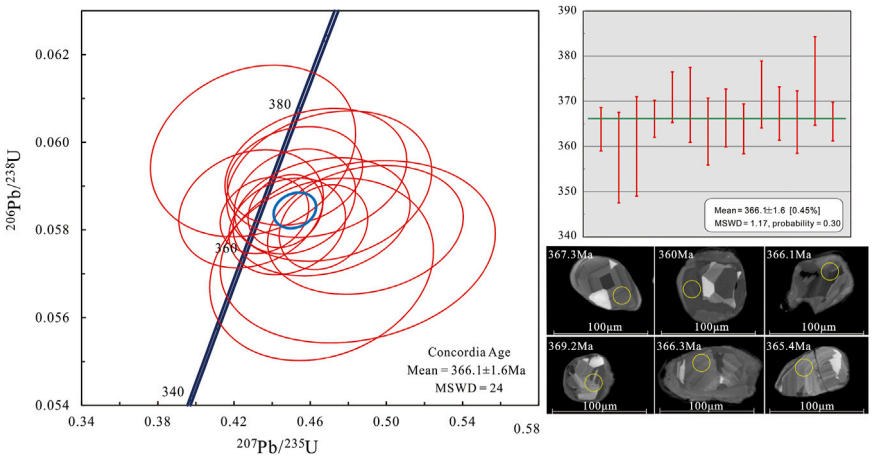

FIGURE 8 | Concordia plot of LA-ICP-MS U–Pb analyses and CL images of zircons from the gabbro in the south margin of Hongshishan intrusion.

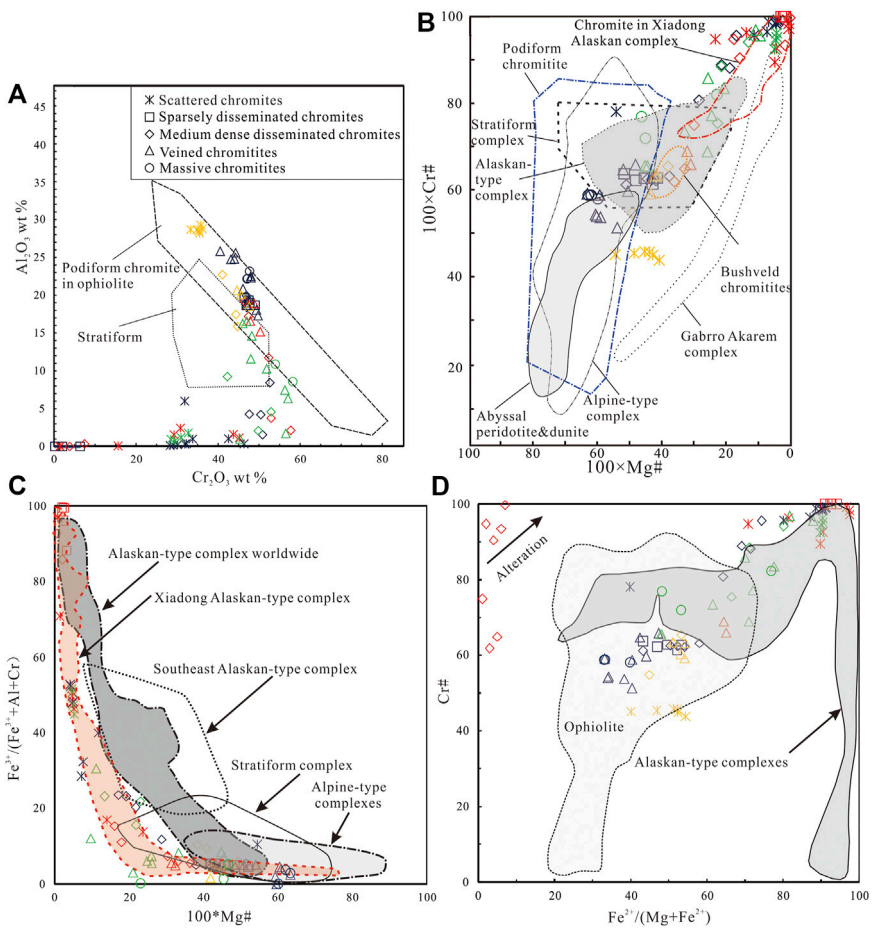

FIGURE 9 | Chromite compositional comparisons of the Hongshishan complex with abyssal peridotites, ophiolites, Alpine-type complex, Bushveld chromites, stratiform complex, and typical Alaskan-type complexes. **(A)** Plot of Al_2O_3 vs. Cr_2O_3 of chromites. Compositional fields of podiform and stratiform chromites are from Bonavia et al. (1993); **(B)** Cr# vs. Mg# diagram of chromites. Compositional fields of abyssal peridotites and dunites are from (Dick and Bullen, 1984); the fields of podiform, stratiform, Alaskan-type complex, Bushveld chromites and Alpine-type field are from Irvine (1967) and Leblanc and Nicolas (1992); the field of the Gabbro Akarem complexes is from Helmy and El Mahallawi (2003); the field of the Xiadong Alaskan complex is from Su et al. (2012); **(C)** Plot of Mg# versus $Fe^{3+}/(Fe^{3+}+Al+Cr)$ of chromites. The field of Alaskan-type complexes worldwide is from Barnes and Roeder (2001); Southeast Alaskan-type complexes, stratiform complexes, and Alpine-type complexes are from Irvine (1967); the Xiadong field is from Su et al. (2012); **(D)** Plot of $Fe^{2+}/(Mg + Fe^{2+})$ vs. Cr# of chromites. The fields of Alaskan-type complexes and ophiolite and alteration trend are after Barnes and Roeder (2001). Different symbol colors correspond to different degrees of magnetization or ferritchromite levels.

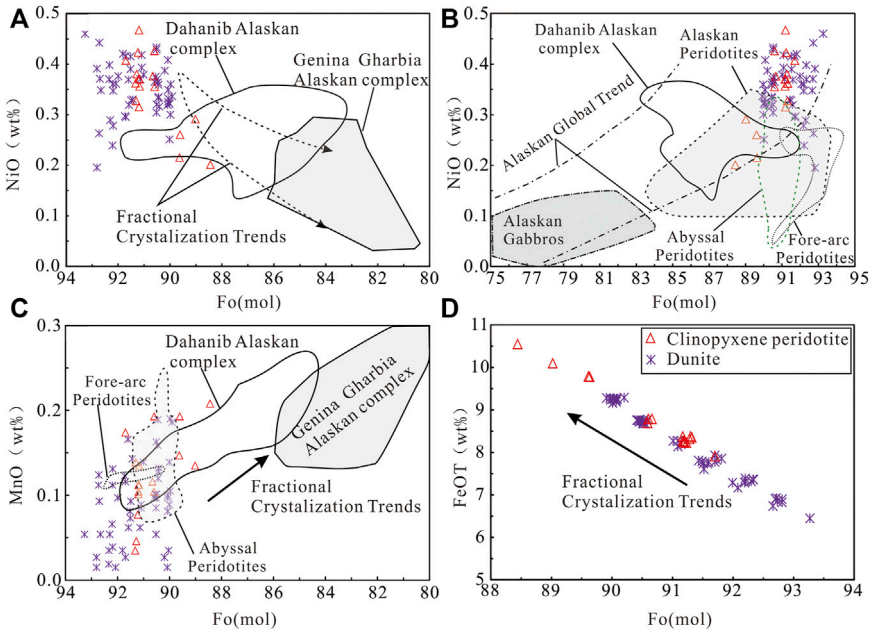

FIGURE 10 | Olivine chemistry of the Hongshishan dunite and clinopyroxene. Plots of Fo versus NiO (wt%), MnO (wt%) showing the olivines following the fractional crystallization trend and Alaskan global trend. The fields of Dahanib and Genina Gharbia are from Khedr et al. (Khedr and Arai., 2016). The fields of the Alaskan global trend and Alaskan gabbros are after Krause et al. (2007), and the fields of Abyssal peridotites and Fore-arc peridotites are from Pagé et al. (2008).

from 2.97 to 70.97 (average 21.72 wt%), FeO from 15.9 to 31.86 (average 23.83 wt%), TiO_2 from 0 to 1.59 (average 0.36wt%), MgO from 0.27 to 14.73 (average 6.19 wt%), and Cr# from 0.44 to 1.0 (0.79 on average) and Mg# from 0 to 0.55 (0.25 on average). A portion of non-magnetized spinels compositions fell inside the field of ophiolitic podiform chromites (**Figures 9A,D**), while plots of Mg# vs. $Fe^{3+}/(Fe^{3+}+Cr+Al)$ and Cr# vs. Fe^{2+}#s (**Figures 9B–D**) show that most data approximate the field of the Alaskan-type complex worldwide and nearly approached the field of the Xiadong Alaskan-type complex (Barnes and Roeder, 2001; Habtoor et al., 2006; Su et al., 2012). The chromites of Hongshishan trend towards Fe^{3+}-rich composition (**Figure 2**), a typical arc-related trend.

Olivines from the dunite are chemically homogeneous, with FeO (average 8.15 wt%), MnO (average 0.09 wt%) and NiO (average 0.35 wt%); they have Forsterite compositions that vary between Fo_{90-93}. Olivines from the clinopyroxene peridotites show slightly higher FeO and MnO levels (average 8.77 and 0.13 wt%, respectively) and the same NiO (average 0.35 wt%). They have Forsterite compositions that vary from Fo_{88-92}, all of which are higher than olivines in Abu Hamamid (Fo_{74-81}), Gabbro-Akarem (Fo_{69-87}), Genina Gharbia (Fo_{80-86}) and Alaskan-type complex (Khedr and Arai., 2016). The Hongshishan olivines plot of NiO, MnO versus Fo falls within in the Alaskan Global trend field but out of the Abyssal peridotite and Fore-arc peridotite fields (**Figures 10B,C**). A graph of FeO_T vs. Fo shows a systematic negative correlation (**Figure 10D**), and a typical fractional crystallization trend similar to olivines in the Alaskan-type complex (**Figures 10A–C**).

The Clinopyroxenes (Cpxs) from the clinopyroxene peridotites are represented by Wo (45–50) and display narrow Mg# (92.4–96.4). The Cpxs contain average amounts of Al_2O_3 (1.07 wt%), Cr_2O_3 (0.31 wt%), FeO (1.99 wt%) and higher amounts of CaO (23.94 wt%). Increased amounts of Al_2O_3 and Na_2O (samples of D01-5-3-1, D01-5-3-2) may be attributed to the neogenic pargasite in diopsides. In the pyroxene classification diagram (**Figure 11A**), nearly all Hongshishan clinopyroxenes fall within the diopside and show similar compositional variations with those of Poshi complexes and Alaskan-type complexes (Su et al., 2013). In the diagram of Al_2O_3 vs. Mg# (**Figure 11B**), most clinopyroxenes from Hongshishan complexes that belong to the second Cpx are similar to those in Alaskan-type intrusions (Khedr and Arai, 2016).

Platinum-Group Elements Geochemistry

Table 1 shows PGE concentrations for all rock types. Total chromite PGE concentrations varied from 17.41 to 218.90 ppb. Just like most ophiolitic podiform chromites, which contain Os, Ir and Ru levels between 0.1 and 0.01 times chondritic (Leblanc 1991) and lower concentrations of Pt and Pd, all samples, except Cr9-11, showed an enriched Ir-subgroup (IPGE = Os, Ir, and Ru) and a depleted Pd-subgroup (PPGE = Rh, Pt, and Pd). The $(Pd/Ir)_N$ ratio of the chromites ranged from 0 to 0.06 (except Cr9-11, Pd/Ir = 8.26) and the chondrite-normalized spider diagram showed steep right-facing sloped patterns, mostly similar to those of the PGE-rich chromites of the Wadi Al Hwanet ophiolite in Saudi Arabia (Ahmed et al., 2012) and the chromitites of the Luobusa ophiolite in Tibet (Zhou et al., 1996) (**Figure 12**).

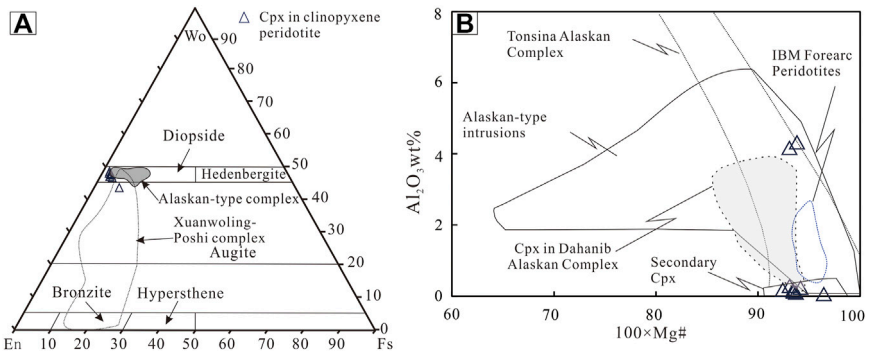

FIGURE 11 | (A) The clinopyroxenes are classified as diopside and plot in the Alaskan-type complex field, the classification triangle diagrams of pyroxenes after Morimoto et al. (Morimoto., 1989). **(B)** Al_2O_3 (wt%) versus Mg# diagrams of Cpxs are similar to Alaskan-type intrusions. The fields of Alaskan-type intrusions, Tonsina Alaskan Complex, and Dahanib intrusion, Secondary Cpx and IBM Forearc Peridotites are from Himmelberg and Loney (1995), DeBari and Coleman (1989), and Khedr et al. (2020), respectively.

TABLE 1 | PGE compositions of whole-rock samples of chromite-bearing dunites in Hongshishan complex.

Sample	Os (ng/g)	Ir (ng/g)	Ru (ng/g)	Rh (ng/g)	Pt (ng/g)	Pd (ng/g)	∑	Pd/Ir
Cr27-b3	6.69	28.90	79.70	5.49	0.74	0.00	121.52	0.00
Cr27-b4	6.81	40.50	105.00	7.93	0.81	1.48	162.53	0.04
Cr27-b5	6.84	48.70	99.70	8.14	0.92	0.87	165.17	0.02
Cr9-B2	24.20	57.00	102.00	7.92	2.40	0.00	193.52	0.00
Cr9-b4	15.00	44.50	86.70	6.71	2.58	0.42	155.91	0.01
Cr9w-B2	13.00	41.70	154.00	8.67	1.53	0.00	218.90	0.00
Cr9-11	0.68	0.91	2.88	0.09	5.33	7.52	17.41	8.26
Cr9-13	4.32	20.60	52.80	4.46	3.18	1.22	86.58	0.06

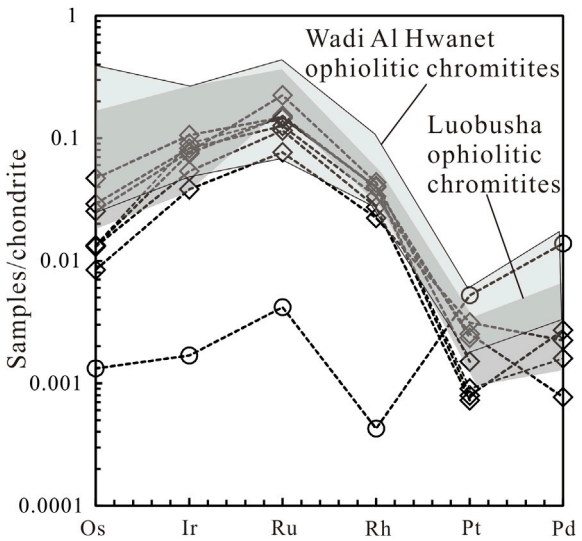

FIGURE 12 | Chondrite-normalized PGE patterns of the chromitites of the Hongshishan complex. The Luobusa ophiolitic chromitite fields (Zhou et al., 1996) and Wadi Al Hwanet ophiolitic chromitites are used for comparison. Normalizing values currently in use are after Naldrett and Duke (1980; cf. 514, 540, 690, 200, 1,020 and 545 for Os, Ir, Ru, Rh, Pt, and Pd, respectively).

DISCUSSION

Texture, Mineralogy, Geochemistry of the Hongshishan Complex and Fractional Crystallization Trends

Petrologically and mineralogically, the Hongshishan complex shows similarities with the Xiadong complex in the Middle Tianshan Terrane (Su et al., 2012; Su et al., 2014) and the Tuerkubantao intrusion in West Junggar (Deng et al., 2015a; Deng et al., 2015b). The Hongshishan complex contains no cross-cutting and intrusive rock unit relationships with distinct geochemical features, this implied the complex was probably not formed by multiple magmatic pulses (Su et al., 2012, 2014). The zonal textural features demonstrated the dunitic core resulted from crystal mush intrusions of deeper-seated cumulate fractionations (Tistl et al., 1994). In our study, compared with Alaskan-type complexes (Irvine, 1974; Himmelberg and Loney, 1995; Krause et al., 2007; Su et al., 2012), the Hongshishan complex has a concentrically zoned structure characterized predominantly by olivine, chrome spinel, clinopyroxene, and hornblende and an absence of orthopyroxene and plagioclase. Nearly all chrome spinels were less hydrous and were free of fluid inclusions, which implied the absence of a magmatic origin of chromite-bearing peridotite silicates in hydrous parental melts or scarce hydrous melts trapped during spinel growth.

Based on field observations, petrography and major element composition variations, the mineral crystallization sequence of the complex proceeded as follows: early cumulus olivine + chrome spinel formed chromite-bearing dunite, followed by crystallization of olivine + chrome spinel + clinopyroxene in spinel-poor clinopyroxene peridotite, and plagioclase + Cpx crystallized to form gabbro (Green et al., 2004; Krause et al., 2007; Khedr et al., 2020).

Generally, the Mg# values of the silicates indicated a fundamental range that followed normal fractional crystallization trends. Moreover, dunites have the highest levels of Ni, Cr, and Mg as compared to other complex units, and probably represented early magmatic products with olivine fractionation (Himmelberg and Loney, 1995). Significantly, from the ultramafic core to the mafic rim, through pyroxenite and the gabbroic margin, the major oxides of the Hongshishan complex have systematically negative correlation trends between major oxides (Al_2O_3, SiO_2, CaO) with Mg# and positive correlations between Mg# with MgO, NiO, and Cr_2O_3; these represent an accumulation of spinel and mafic minerals and the change of fractional crystallization degrees from the ultramafic core outwards from a common parental magma chamber of Uralian–Alaskan-type complex (Himmelberg and Loney, 1995; Farahat and Helmy, 2006; Habtoor et al., 2016).

For Uralian–Alaskan-type complexes, decreases in Fo and Cr# in the coexisting chromite helped monitor the early olivine and chromite crystallization stages. Olivine fractionation was significant during the early stage of magma ascension and evolution, as Mg preferentially partitioned into olivine accumulation instead of coexisting in a melt or other silicate minerals (Green et al., 2004; Teng, 2017). Crystallization of large olivine amounts to form an olivine-rich peridotite enriched the parental melt with Cr, Fe, and Al and triggered the crystallization of Fe, Al-rich chromite to form chromite. Crystallization of the chromite, and vice versa, increased magma Mg levels. High Fo values in olivine and the high Cr/(Cr + Al) in the spinel implied a parental magma rich in MgO but poor in Al_2O_3 (Krause et al., 2007). Additionally, increased Fe and Mn levels in dunite olivines to the one in the spinel-poor clinopyroxene peridotite likely relates to fractional crystallization (Khedr et al., 2020). Diagrams of major oxides versus Fo for olivines in dunite and clinopyroxene peridotite from the Hongshishan complex appeared within the Alaskan Global trend fields and showed a typical fractional crystallization trend similar to olivines in typical Alaskan-type complexes (**Figure 10**).

The Chondrite-normalized rare Earth element patterns are shown in **Figure 7**. All samples showed highly variable concentrations of HREE but slight enrichments of total REE levels and other incompatible elements relative to primitive mantle values from the ultramafic core to the marginal gabbroic rocks. The strong positive anomalies of Ba and Sr and the slight positive Eu anomaly from gabbros and pyroxenite whole rock samples supported a cumulative origin, i.e., accumulation of plagioclase. The REE patterns of the peridotites depended on the melting degree and mineralogy involved when the initial residue and enriched melt were formed. Residue composition formed by varying degrees of non-modal fractional melting of the same source. LREE-enriched patterns developed if melting occurred in the spine1 stability field. U-shaped REE patterns represent mixing of these residues with different degrees of incipient melts (Song and Frey, 1989). Additionally, serpentinization, carbonation, and hydrous fluid metasomawotism by LREE-enriched melts act as primary causes of LREE/HREE fractionation, LREE enrichment in carbonated peridotite rocks (Becker et al., 2001; Tian et al., 2011; Boskabadi et al., 2020), and subduction-related fluid, melts necessarily account for LILE-enrichment and HFSE-depletion of peridotite rocks in this complex.

Our preliminary investigation, combining the current field survey with these new observations, revealed that the petrological and mineralogical features of the Hongshishan complex were comparable with a Ural–Alaskan type complex.

Crustal Contamination

Even though interactions with late interstitial, percolating melts, fluids, and subsolidus equilibration with neighboring grains can modify the elemental concentration in minerals as well as the mineral composition in cumulate rocks (Krause et al., 2007; Murphy, 2013); however, we did not observe any evidence of percolation and melt-rock reactions in the field or on a microscopic scale. Additionally, even though crustal contamination potentially increases Th/Yb ratios and reduces Nb/La, Ta/La, and Nb/Th ratios (Neal et al., 2002; Pearce, 2008), negative Eu anomalies and REE fractionation may imply crustal assimilation. Because the trace and REE element patterns of ultramafic cores and the marginal gabbros have sub-parallel trends, it implied that the different rock types of the Hongshishan complex are comagmatic, and

initially generated by fractional crystallization from a common basaltic melt. The negative Eu anomalies of dunite accompanied by LREE enrichment were interpreted by a disequilibrium melting model, when and where, melting began in the garnet lherzolite facies through the spinel facies and concluded in the plagioclase facies. Phases in the source melted; however, the melt did not equilibrate with residual minerals. The negative Eu anomalies meant that some partial melting occurred in the plagioclase facies. Disequilibrium melting of plagioclase produces a residue with a negative Eu anomaly because of the positive Eu anomaly caused by suppressed crystallization of plagioclase (Prinzhofer and Allègre, 1985; McDonough and Frey, 1989; Wang et al., 1996). In addition, the absence of plagioclase in dunite and clinopyroxene peridotite likely caused the negative Eu anomaly due to low Sr concentrations, and subsequent serpentinization, carbonatization and metasomatism related subduction resulted in the higher total REE abundance, LREE enrichment with negative dunite Eu anomalies.

Cr-spinels in Hongshishan dunites showed $^{187}Os/^{188}Os$ isotopic ratios from 0.1251 to 0.1274 and $^{187}Re/^{188}Os$ ratios from 0.0066 to 0.0842. The Re/Os isotopic compositions of Cr-spinel samples appeared in the chromite field, which represents a residual peridotites trend. Just like a Gaositai complex with no significant crustal contamination in North China (Tian et al., 2011), the mean $^{187}Os/^{188}Os$ ratio for the chromites from Hongshishan showed that magmas originated from the mantle. The radiogenic Os isotopic compositions of the chromites meant the parental magmas of the Hongshishan complex suffered minor contamination coming from crustal components during magma volution. So crustal assimilation may not be necessary to significantly change the geochemical compositions of the parental magmas (Reiners et al., 1996; Batanova et al., 2005; Burg et al., 2009; Su et al., 2014).

Possible Tectonic Setting of the Hongshishan Alaskan-type Complex

Tectonically, some researchers have proposed that Alaskan-type complexes formed at subduction zones, representing arc magmas (Taylor, 1967; Irvine, 1974; Helmy and El Mahallawi, 2003), arc-root complexes (DeBari and Coleman, 1989; Brugmann et al., 1997; Helmy et al., 2014), at the change from the arc setting to the extensional regime (Tistl et al., 1994; Mues-Schumacher et al., 1996; Chen et al., 2009; Tian et al., 2011; Spandler and Pirard, 2013; Helmy et al., 2015) or even related to mantle plume (Ishiwatari and Ichiyama, 2004; Pirajno, 2004; Farahat and Helmy, 2006).

The Alaskan-type complexes of Xiadong in Central Tianshan and Tuerkubantao in West Junggar are arc-related, and interpreted as the product of partial melting of metasomatized lithospheric mantle triggered by subduction of an oceanic plate or slab window created by the subduction of an oceanic ridge (Xiao et al., 2010; Su et al., 2012; Su et al., 2014; Deng et al., 2015a; Deng et al., 2015b). In the early Carboniferous, Hongshishan, Liutuoshan areas might have evolved into an initial small oceanic basin (Zuo et al., 1990a; Zuo et al., 1990b; Zhao et al., 1994; Wang et al., 2014), but had not reached the degree of a mature mid-ocean ridge (Gong et al., 2003; Huang and Jin, 2006a; Huang and Jin, 2006b; Shi et al., 2017) because the geochemistries and age data came from basalts and gabbros in the Carboniferous Lvtiaoshan Formation, characterized by the occurrence of the bimodal volcanic rocks and lack of data on the mafic and ultramafic rocks in the complex (Peng et al., 2016). Virtually, the Hongshishan ultramafic-mafic complex lacked mantle peridotite, mafic cumulate, as well as pillow lava, so the ultramafic and mafic rocks were not the member compositions of a typical ophiolite (Yang et al., 2010; Wang et al., 2013; Peng et al., 2016).

We deduced that subduction or an arc magma setting could account for the upwelling of the depleted asthenosphere and rapid ascending magma flow which was less hydrous or free of opaque inclusions. Os isotopic compositions of chromian spinels in chromite suggested minor magma crustal contaminations. Formation of chromite was thought of as related to the evolution and chemical composition change of the parent magma (Tian et al., 2011). We attributed the enriched Fe^{3+} chromite compositions, LILE-enrichment, and HFSE-depletion of peridotite rocks and the neogenic clinopyroxenes in the clinopyroxene peridotites to suffering subduction modification and enrichment.

Chromite and PGE Mineralization

In the Alaskan-type complexes, chromites occurred as bands, seams, massive, veined or disseminated, and were accompanied by cumulate dunites (Himmelberg and Loney, 1995; Garuti et al., 2002; Garuti et al., 2003; Krause et al., 2007; Tian et al., 2011; Khedr et al., 2020). Cumulus olivines in host dunites and banded chromites with varying degrees of disseminated chromian-spinel grains were the typical characters of fractional crystallization (Khedr et al., 2020). Chromites may enter clinopyroxene crystals in an isomorphic form instead of an olivine form and crystalize in a chromian-spinel form during cumulation of olivine, so chromites form in cumulate dunite rather than in clinopyroxene-riched rocks. As the olivines fractionally crystallized, chromite compositions and relatively volatile components concentrated in residual magma. The emergence of high concentrations of volatiles largely delayed melt crystallization times and promoted the formation of ore pulp from ore-forming components as a massive and veined chromite orebody. Thus, those two different processes accounted for chromite formation, where the former crystallized from melting and released chrome-bearing minerals, which accumulated through fractional crystallization. In the latter, ore pulps carried by volatiles cut across the earlier disseminated chromite ores. The textures in Hongshishan chromites show that the disseminated chromite crystallized earlier than the massive and veined chromites. The Uralian-Alaskan-type chromites are characterized by the predominant composition of $Cr^{3+} \rightarrow Fe^{3+}$ substitution, which indicated an oxygen fugacity (fO_2) variation during chromite precipitation (Johan, 2006). Crystallization and separation of Alaskan-type magma at high oxygen fugacity promoted transformation of the magma Fe^{2+} components into Fe^{3+}, which impeded the

combination of FeO with MgO and SiO_2 to produce poor a CaO-poor orthopyroxene, which instead occurred as magnetite and dispersed throughout the magma to form an iron-rich cumulatite.

Alaskan-type complexes are well-known as sub-economic Cu–Ni–PGE mineralization hosts, other than chromite deposits (Helmy and Mogessie, 2001; Helmy, 2004). However, the parental magmas of Alaskan-type complexes are water-rich/hydrous with high oxygen fugacities and less crustal assimilation, which might explain the absence of Ni–Cu sulfide mineralization that requires a reducing environment for most Alaskan-type complexes (Pettigrew and Hattori, 2006; Su et al., 2013). The Hongshishan complex contains a unique Ir-Ru-rich chromite deposit along the southern border of the Altaids orogenic belt. The first PGE-bearing sulfides crystallized within the early cumulus olivine and chromian spinels as primary inclusions with variable but generally high levels of PGE (17.41–218.90 ppb). They display similar patterns with IPGE enrichment (Os, Ir, Ru), PPGE depletion (Pt, Pd), and Ni/Cu depletions. Partial melting of the upper mantle controls PGE levels and their distribution in mantle rocks, and the migrating ability of IPGE is significantly weaker than PPGE (Wood, 1987; Zhou et al., 2014). IPGEs are compatible elements in monosulfide solid solutions (MSS), while PPGEs are incompatible with MSS when MSS forms by fractional crystallization of sulfide melts. High levels of IPGEs occurred in MSS whereas PPGE increased in residual sulfide melts, leading to the differentiation of PGE (Mungall et al., 2005; Cui et al., 2020).

PGE-bearing chromite mineralization in addition to the Hongshishan complex has not been reported in a mafic-ultramafic complex along the southern border of the Altaids orogenic belt. The identification of the Hongshishan Alaskan-type complex indicated that this kind of complex has great potential for chrome-PGE prospecting in the Beishan orogenic collage.

CONCLUSION

1) The Hongshishan mafic-ultramafic complex shows concentric zonation, from clinopyroxene peridotite and dunite in the core to mafic intrusions, including pyroxenite and gabbro in the margin.
2) Systematic trends among the major element oxides and chemical compositions of spinel, olivine, and clinopyroxenes suggested fractional crystallization. The absence of orthopyroxene and the fact that nearly all chrome spinels were less hydrous and free of fluid inclusions meant a magmatic origin of chromite-bearing peridotites was absent in hydrous parental melts or scarce hydrous melts. Subduction modification and enrichment, together with serpentinization and carbonatization, may explain the LILE-enrichment and HFSE-depletion of peridotite rocks in this complex. Crustal assimilation may not directly explain negative Eu anomalies and REE fractionation of mafic-ultramafic rocks. The complexes share similar petrological, geochemical, and mineralogical features with typical Alaskan-type complexes.
3) The Hongshishan complex contains a unique Ir-Ru-rich chromite deposit along the southern border of the Altaids orogenic belt. The chromites are enriched in IPGE and a chondrite-normalized spider diagram showed steep right-facing sloped patterns, which approximated those of PGE-rich ophiolitic chromites.
4) Tectonically, the Hongshishan complex is neither an ophiolite remnant nor a stratiform mafic-ultramafic intrusion, but rather an Alaskan-type intrusion related to subduction or arc magmas and approximately 366.1 Ma years old and suffered subduction modification and enrichment.

DATA AVAILABILITY STATEMENT

The original contributions presented in the study are included in the article/**Supplementary Material**, further inquiries can be directed to the corresponding authors.

AUTHOR CONTRIBUTIONS

All authors listed have made a substantial, direct, and intellectual contribution to the work and approved it for publication.

FUNDING

This research was jointly supported by the National Key Research and Development Program of China (No. 2018YFC0604002), China Geological Survey (Nos. DD20190071, DD20190812), and the Basic Science Foundation of CAGS, China (No. JKY21021).

ACKNOWLEDGMENTS

The authors thank the reviewers for their thorough, critical, and constructive reviews and comments. We are also grateful to Prof. Yufeng Deng for their helpful discussions and suggestions.

SUPPLEMENTARY MATERIAL

The Supplementary Material for this article can be found online at: https://www.frontiersin.org/articles/10.3389/feart.2021.663760/full#supplementary-material

REFERENCES

Ahmed, A. H., Harbi, H. M., and Habtoor, A. M. (2012). Compositional variations and tectonic settings of podiform chromitites and associated ultramafic rocks of the Neoproterozoic ophiolite at Wadi Al Hwanet, northwestern Saudi Arabia. *J. Asian Earth Sci.* 56, 118–134.

Ao, S. J., Xiao, W. J., Han, C. M., Mao, Q. G., and Zhang, J. E. (2010). Geochronology and Geochemistry of Early Permian Mafic-Ultramafic Complexes in the Beishan Area, Xinjiang, NW China: Implications for Late

Paleozoic Tectonic Evolution of the Southern Altaids. *Gondwana Res.* 18 (2–3), 466–478. doi:10.1016/j.gr.2010.01.004

Barnes, S. J., and Roeder, P. L. (2001). The Range of Spinel Compositions in Terrestrial Mafic and Ultramafic Rocks. *J. Pet.* 42, 2279–2302. doi:10.1093/petrology/42.12.2279

Batanova, V. G., Pertsev, A. N., Kamenetsky, V. S., Ariskin, A. A., Mochalov, A. G., and Sobolev, A. V. (2005). Crustal Evolution of Island-Arc Ultramafic Magma: Galmoenan Pyroxenite-Dunite Plutonic Complex, Koryak Highland (Far East Russia). *J. Pet.* 46, 1345–1366. doi:10.1093/petrology/egi018

Becker, H., Shirey, S. B., and Carlson, R. W. (2001). Effects of Melt Percolation on the Re-os Systematics of Peridotites from a Paleozoic Convergent Plate Margin. *Earth Planet. Sci. Lett.* 188, 107–121. doi:10.1016/s0012-821x(01)00308-9

Bonavia, F. F., Diella, V., and Ferrario, A. (1993). Precambrian Podiform Chromites from Kenticha Hill, Southern Ethiopia. *Econ. Geology.* 88, 198–202. doi:10.2113/gsecongeo.88.1.198

Boskabadi, A., Pitcairn, I. K., Leybourne, M. I., Teagle, D. A. H., Cooper, M. J., Hadizadeh, H., et al. (2020). Carbonation of Ophiolitic Ultramafic Rocks: Listvenite Formation in the Late Cretaceous Ophiolites of Eastern Iran. *Lithos*, 352–353. doi:10.1016/j.lithos.2019.105307

Brügmann, G. E., Reischmann, T., Naldrett, A. J., and Sutcliffe, R. H. (1997). Roots of an Archean volcanic arc complex: the Lac des Iles area in Ontario, Canada. *Precambrian Res.* 81, 223–239. doi:10.1016/S0301-9268(96)00036-8

Burg, J.-P., Bodinier, J.-L., Gerya, T., Bedini, R.-M., Boudier, F., Dautria, J.-M., et al. (2009). Translithospheric Mantle Diapirism: Geological Evidence and Numerical Modelling of the Kondyor Zoned Ultramafic Complex (Russian Far-East). *J. Pet.* 50, 289–321. doi:10.1093/petrology/egn083

Chen, B., Suzuki, K., Tian, W., Jahn, B. M., and Ireland, T. (2009). Geochemistry and Os-Nd-Sr Isotopes of the Gaositai Alaskan-type Ultramafic Complex from the Northern North China Craton: Implications for Mantle-Crust Interaction. *Contrib. Mineral. Petrol.* 158, 683–702. doi:10.1007/s00410-009-0404-7

Cui, M. M., Su, B. X., Wang, J., Chen, K. Y., and Gao, D. L. (2020). Alaskan-type Nature and Pge Mineralization of the Wuxing Mafic-Ultramafic Complex in Eastern Part of the central Asian Orogenic belt. *Ore Geo. Rev.* 123, 10356. doi:10.1016/j.oregeorev.2020.103566

DeBari, S. M., and Coleman, R. G. (1989). Examination of the Deep Levels of an Island Arc: Evidence from the Tonsina Ultramafic-Mafic Assemblage, Tonsina, Alaska. *J. Geophys. Res.* 94, 4373–4391. doi:10.1029/jb094ib04p04373

Deng, Y.-F., Yuan, F., Zhou, T., White, N. C., Zhang, D., Guo, X., et al. (2015b). Zircon U-Pb Geochronology, Geochemistry, and Sr-Nd Isotopes of the Ural-Alaskan Type Tuerkubantao Mafic-Ultramafic Intrusion in Southern Altai Orogen, China: Petrogenesis and Tectonic Implications. *J. Asian Earth Sci.* 113, 36–50. doi:10.1016/j.jseaes.2015.05.007

Deng, Y., Yuan, F., Zhou, T., Xu, C., Zhang, D., and Guo, X. (2015a). Geochemical Characteristics and Tectonic Setting of the Tuerkubantao Mafic-Ultramafic Intrusion in West Junggar, Xinjiang, China. *Geosci. Front.* 6, 141–152. doi:10.1016/j.gsf.2013.10.003

Dick, H. J. B., and Bullen, T. (1984). Chromian spinel as a petrogenetic indicator in abyssal and alpine-type peridotites and spatially associated lavas. *Contrib. Mineral. Petrol.* 86, 54–76.

Efimov, A. A. (1998). The Platinum belt of the Urals: Structure, Petrogenesis, and Correlation with Platiniferous Complexes of the Aldan Shield and Alaska. Abstr 8th Intern Platinum Symp, South Africa, June 29-July 2, 1998, 93–96.

Farahat, E. S., and Helmy, H. M. (2006). Abu Hamamid Neoproterozoic Alaskan-type Complex, South Eastern Desert, Egypt: Petrogenetic and Geotectonic Implications. *J. Afr. Earth Sci.* 45, 187–197. doi:10.1016/j.jafrearsci.2006.02.003

Foley, J. P., Light, T. D., Nelson, S. W., and Harris, R. A. (1997). Mineral Occurrences Associated with Mafic-Ultramafic and Related Alkaline Complexes in Alaska. *Econ. Geology.* 9, 396–449.

Garuti, G., Pushkarev, E. V., Zaccarini, F., Cabella, R., and Anikina, E. (2003). Chromite Composition and Platinum-Group mineral Assemblage in the Uktus Uralian–alaskan-type Complex (Central Urals, Russia). *Can. Mineral.* 38, 312–326. doi:10.1007/s00126-003-0348-1

Garuti, G., Pushkarev, E. V., and Zaccarini, F. (2002). Composition and Paragenesis of Pt Alloys from Chromites of the Uralian–alaskan-type Kytlym and Uktus Complexes, Northern and central Urals, Russia. *Can. Mineral.* 40, 1127–1146. doi:10.2113/gscanmin.40.4.1127

Gong, Q. S., Liu, M. Q., and Liang, M. H. (2003). The Tectonic Facies and Tectonic Evolution of Beishan Orogenic belt. *Gansu. Northwest. Geology.* 36 (1), 11–17. (in Chinese with English abstract).

Green, D. H., Schmidt, M. W., and Hibberson, W. O. (2004). Island-arc Ankaramites: Primitive Melts from Fluxed Refractory Lherzolitic Mantle. *J. Pet.* 45, 391–403. doi:10.1093/petrology/egg101

Greenbaum, D. (1977). The Chromitiferous Rocks of the Troodos Ophiolite Complex, Cyprus. *Econ. Geology.* 72, 1175–1194. doi:10.2113/gsecongeo.72.7.1175

Guo, Q., Xiao, W., Windley, B. F., Mao, Q., Han, C., Qu, J., et al. (2012). Provenance and Tectonic Settings of Permian Turbidites from the Beishan Mountains, NW China: Implications for the Late Paleozoic Accretionary Tectonics of the Southern Altaids. *J. Asian Earth Sci.* 49, 54–68. doi:10.1016/j.jseaes.2011.03.013

Habtoor, A., Ahmed, A. H., and Harbi, H. (2016). Petrogenesis of the Alaskan-type Mafic-Ultramafic Complex in the Makkah Quadrangle, Western Arabian Shield, Saudi Arabia. *Lithos* 263, 33–51. doi:10.1016/j.lithos.2016.08.014

He, S. P., Zhou, H. W., Ren, B. C., Yao, W. G., and Fu, L. P. (2005). Crustal Evolution of Paleozoic in Beishan Area, Gansu and Inner Mongolia, China. *Northwest. Geology.* 38 (3), 6–15. (in Chinese with English abstract).

Helmy, H. M., Abd El-Rahman, Y. M., Yoshikawa, M., Shibata, T., Arai, S., Tamura, A., et al. (2014). Petrology and Sm-Nd Dating of the Genina Gharbia Alaskan-type Complex (Egypt): Insights into Deep Levels of Neoproterozoic Island Arcs. *Lithos* 198-199, 263–280. doi:10.1016/j.lithos.2014.03.028

Helmy, H. M. (2004). Cu Ni PGE Mineralization in the Genina Gharbia Mafic Ultramafic Intrusion, Eastern Desert, egypt. *The Can. Mineralogis* 42, 351–370. doi:10.2113/gscanmin.42.2.351

Helmy, H. M., and El Mahallawi, M. M. (2003). Gabbro Akarem Mafic-Ultramafic Complex, Eastern Desert, Egypt: a Late Precambrian Analogue of Alaskan-type Complexes. *Mineralogy Pet.* 77, 85–108. doi:10.1007/s00710-001-0185-9

Helmy, H. M. (2005). Melonite Group Minerals and Other Tellurides from Three Cu-Ni-PGE Prospects, Eastern Desert, Egypt. *Can. Mineral.* 42, 305–324. doi:10.2113/gscanmin.42.2.351

Helmy, H. M., and Mogessie, A. (2001). Gabbro Akarem, Eastern Desert, Egypt: Cu-Ni-PGE Mineralization in a Concentrically Zoned Mafic-Ultramafic Complex. *Mineralium Deposita* 36, 58–71. doi:10.1007/s001260050286

Helmy, H. M., Yoshikawa, M., Shibata, T., Arai, S., and Kagami, H. (2015). Sm-Nd and Rb-Sr Isotope Geochemistry and Petrology of Abu Hamamid Intrusion, Eastern Desert, Egypt: An Alaskan-type Complex in a Backarc Setting. *Precambrian Res.* 258, 234–246. doi:10.1016/j.precamres.2015.01.002

Himmelberg, G. R., and Loney, R. A. (1995). Characteristics and Petrogenesis of Alaskan-type Ultramafic–Mafic Intrusions, southeastern Alaska. USGS, U.S. Geological Survey Professional Paper 1564.

Huang, Z. B., and Jin, X. (2006a). Tectonic Environment of Basic Volcanic Rocks in the Hongshishan Ophiolite Melange Zone, Beishan Mountains. *Gansu.Geology in China* 33 (5), 1030–1037. (in Chinese with English abstract).

Huang, Z. B., and Jin, X. (2006b). Geochemistry Features and Tectonic Setting of the Hongshishan Ophiolite in. *Gansu Province. Chin. J. Geology.* 41 (4), 601–611. (in Chinese with English abstract).

Huang, Z. B., and Jin, X. (2006c). Geological Characteristics and its Setting for Volcanic Rocks of Baishan Formation in Hongshishan Area of Gansu Province. *Gansu Geology.* 15, 19–24. (in Chinese with English abstract).

Irvine, T. N. (1967). Chromian Spinel as a Petrogenetic Indicator. Part II. Petrogenetic Applications. *Can. J. earth Sci.* 11 (4), 71–103. doi:10.1139/e67-004

Irvine, T. N. (1974). Petrology of the Duke Island ultramafic complex, southeastern Alaska. *Geol. Soc. Amer. Memo.* 138, 1–240.

Ishiwatari, A., and Ichiyama, Y. (2004). Alaskan-Type Plutons and Ultramafic Lavas in Far East Russia, Northeast China, and Japan. *Int. Geology. Rev.* 46, 316–331. doi:10.2747/0020-6814.46.4.316

Johan, Z. (2006). Platinum-group Minerals from Placers Related to the Nizhni Tagil (Middle Urals, Russia) Uralian-alaskan-type Ultramafic Complex: Ore-Mineralogy and Study of Silicate Inclusions in (Pt, Fe) Alloys. *Mineralogy Pet.* 87, 1–30. doi:10.1007/s00710-005-0117-1

Khedr, M. Z., Arai, S., and Morishita, T. (2020). Formation of Banded Chromitites and Associated Sulphides in the Neoproterozoic Subarc Deep-Crustal Magma Inferred from the Alaskan-type Complex, Egypt. *Ore Geology. Rev.* 120, 103410. doi:10.1016/j.oregeorev.2020.103410

Khedr, M. Z., and Arai, S. (2016). Petrology of a Neoproterozoic Alaskan-type Complex from the Eastern Desert of Egypt: Implications for Mantle Heterogeneity. *Lithos* 263, 15–32. doi:10.1016/j.lithos.2016.07.016

Krause, J., Brügmann, G. E., and Pushkarev, E. V. (2007). Accessory and Rock Forming Minerals Monitoring the Evolution of Zoned Mafic-Ultramafic Complexes in the Central Ural Mountains. *Lithos* 95, 19–42. doi:10.1016/j.lithos.2006.07.018

Leblanc, M., and Nicolas, A. (1992). Ophiolitic Chromitites. *Int. Geology. Rev.* 34, 653–686. doi:10.1080/00206819209465629

Leblanc, M. (1991). "Platinum-Group Elements and Gold in Ophiolitic Complexes: Distribution and Fractionation from Mantle to Oceanic Floor," in *Ophwliie Genesis and Evolution of the Oceanic Lithosphere*. Editors T Peters, A. Nicolas, and R. G. Coleman (Dordrecht: Kluwer Academic), 231–260. doi:10.1007/978-94-011-3358-6_13

Liu, X., and Wang, Q. (1995). Tectonics and Evolution of the Beishan Orogenic belt. West China. *Geol. Res.* 10, 151–165.

Mao, Q., Xiao, W., Windley, B. F., Han, C., Qu, J., Ao, S., et al. (2012). The Liuyuan Complex in the Beishan, NW China: a Carboniferous-Permian Ophiolitic Fore-Arc Sliver in the Southern Altaids. *Geol. Mag.* 149, 483–506. doi:10.1017/s0016756811000811

McDonough, W. F., and Frey, F. A. (1989). Rare Earth Elements in Upper Mantle Rocks. *Rev. Mineralogy Geochem.* 21, 100–145.

McDonough, W. F., and Sun, S. S. (1995). The Composition of the Earth. *Chem. Geology.* 120 (3–4), 223–253. doi:10.1016/0009-2541(94)00140-4

Morimoto, N. (1989). Nomenclature of Pyroxenes. *Can. Mineral.* 27, 143–156. doi:10.2465/minerj.14.198

Mues-Schumacher, U., Keller, J., Kononova, V. A., and Suddaby, P. J. (1996). Mineral Chemistry and Geochronology of the Potassic Alkaline Ultramafic Inagli Complex, Aldan Shield, Eastern Siberia. *Mineral. Mag.* 60, 711–730. doi:10.1180/minmag.1996.060.402.02

Mungall, J. E., Andrews, D. R. A., Cabri, L. J., Sylvester, P. J., and Tubrett, M. (2005). Partitioning of Cu, Ni, Au, and Platinum-Group Elements between Monosulfide Solid Solution and Sulfide Melt under Controlled Oxygen and Sulfur Fugacities. *Geochimica et Cosmochimica Acta* 69, 4349–4360. doi:10.1016/j.gca.2004.11.025

Murphy, J. B. (2013). Appinite Suites: a Record of the Role of Water in the Genesis, Transport, Emplacement and Crystallization of Magma. *Earth-Science Rev.* 119, 35–59. doi:10.1016/j.earscirev.2013.02.002

Neal, C. R., Mahoney, J. J., and Chazey, W. J., III (2002). Mantle Sources and the Highly Variable Role of Continental Lithosphere in Basalt Petrogenesis of the Kerguelen Plateau and Broken Ridge LIP: Results from ODP Leg 183. *J. Pet.* 43, 1177–1205. doi:10.1093/petrology/43.7.1177

Pagé, P., Bédard, J. H., Schroetter, J.-M., and Tremblay, A. (2008). Mantle Petrology and Mineralogy of the Thetford Mines Ophiolite Complex. *Lithos* 100, 255–292. doi:10.1016/j.lithos.2007.06.017

Pearce, J. A. (2008). Geochemical Fingerprinting of Oceanic Basalts with Applications to Ophiolite Classification and the Search for Archean Oceanic Crust. *Lithos* 100, 14–48. doi:10.1016/j.lithos.2007.06.016

Peng, X. P., Chen, G. C., Li, Y. H., Li, J. C., Jiang, T., Shi, J. Z., et al. (2016). Ophiolite Mélange belt Composition and Geologic Significance of Hongshishan in Beishan Area. *Xinjiang Geol.* 34 (2), 184–191. (in Chinese with English abstract).

Pettigrew, N. T., and Hattori, K. H. (2006). The Quetico Intrusions of Western Superior Province: Neo-Archean Examples of Alaskan/Ural-type Mafic-Ultramafic Intrusions. *Precambrian Res.* 149, 21–42. doi:10.1016/j.precamres.2006.06.004

Pirajno, F. (2004). Hotspots and Mantle Plumes: Global Intraplate Tectonics, Magmatism and Ore Deposits. *Mineralogy Pet.* 82, 183–216. doi:10.1007/s00710-004-0046-4

Prinzhofer, A., and Allègre, C. J. (1985). Residual Peridotites and the Mechanisms of Partial Melting. *Earth Planet. Sci. Lett.* 74, 251–265. doi:10.1016/0012-821x(85)90025-1

Reiners, P. W., Nelson, B. K., and Nelson, S. W. (1996). Evidence for Multiple Mechanisms of Crustal Contamination of Magma from Compositionally Zoned Plutons and Associated Ultramafic Intrusions of the Alaska Range. *J. Pet.* 37, 261–292. doi:10.1093/petrology/37.2.261

Ripley, E. M. (2009). "Magmatic Sulfide Mineralization in Alaskan-type Complexes," in *New Development in Magmatic Ni-Cu and PGE Deposits 7*. Editors C.S. Li and E.M. Ripley (Beijing: Geological Publishing House), 219–228.

Saleeby, J. B. (1992). Age and Tectonic Setting of the Duke Island Ultramafic Intrusion, Southeast Alaska. *Can. J. Earth Sci.* 29, 506–522. doi:10.1139/e92-044

Sha, L.-K. (1995). Genesis of Zoned Hydrous Ultramafic/mafic-Silicic Intrusive Complexes: an MHFC Hypothesis. *Earth-Science Rev.* 39, 59–90. doi:10.1016/0012-8252(95)00002-r

Shi, Y., Li, L., Kröner, A., Ding, J., Zhang, W., Huang, Z., et al. (2017). Carboniferous Alaskan-type Complex along the Sino-Mongolian Boundary, Southern Margin of the Central Asian Orogenic Belt. *Acta Geochim* 36 (2), 276–290. doi:10.1007/s11631-017-0145-7

Shi, Y., Zhang, W., Kröner, A., Li, L., and Jian, P. (2018). Cambrian Ophiolite Complexes in the Beishan Area, China, Southern Margin of the Central Asian Orogenic Belt. *J. Asian Earth Sci.* 153, 193–205. doi:10.1016/j.jseaes.2017.05.021

Snoke, A. W., Quick, J. E., and Bowman, H. R. (1981). Bear Mountain Igneous Complex, Klamath Mountains, California: an Ultrabasic to Silicic Cale-Alkaline Suite. *J. Pet.* 22, 501–552. doi:10.1093/petrology/22.4.501

Song, D., Xiao, W., Windley, B. F., Han, C., and Tian, Z. (2015). A Paleozoic Japan-type Subduction-Accretion System in the Beishan Orogenic Collage, Southern Central Asian Orogenic Belt. *Lithos* 224-225, 195–213. doi:10.1016/j.lithos.2015.03.005

Song, Y., and Frey, F. A. (1989). Geochemistry of Peridotite Xenoliths in basalt from Hannuoba, Eastern china: Implications for Subcontinental Mantle Heterogeneity. *Geochimica et Cosmochimica Acta* 53 (1), 97–113. doi:10.1016/0016-7037(89)90276-7

Spandler, C., and Pirard, C. (2013). Element Recycling from Subducting Slabs to Arc Crust: a Review. *Lithos* 170-171, 208–223. doi:10.1016/j.lithos.2013.02.016

Su, B.-X., Qin, K.-Z., Sakyi, P. A., Malaviarachchi, S. P. K., Liu, P.-P., Tang, D.-M., et al. (2012). Occurrence of an Alaskan-type Complex in the Middle Tianshan Massif, Central Asian Orogenic Belt: Inferences from Petrological and Mineralogical Studies. 54, 249–269.doi:10.1080/00206814.2010.543009

Su, B.-X., Qin, K.-Z., Zhou, M.-F., Sakyi, P. A., Thakurta, J., Tang, D.-M., et al. (2014). Petrological, Geochemical and Geochronological Constraints on the Origin of the Xiadong Ural-Alaskan Type Complex in NW China and Tectonic Implication for the Evolution of Southern Central Asian Orogenic Belt. *Lithos* 200-201, 226–240. doi:10.1016/j.lithos.2014.05.005

Su, B. X., Qin, K. Z., Santosh, M., Sun, H., and Tang, D. M. (2013). The Early Permian Mafic–Ultramafic Complexes in the Beishan Terrane, NW China: Alaskan-type Intrusives or Rift Cumulates? *Int. Geology. Rev.* 66, 175–187. doi:10.1016/j.jseaes.2012.12.039

Sun, S. S., and McDonough, W. F. (1989). Chemical and Isotopic Systematics of Oceanic Basalts: Implications for Mantle Composition and Processes. *Geol. Soc. Lond. Spec. Publications* 42 (1), 313–345. doi:10.1144/gsl.sp.1989.042.01.19

Taylor, H. P. (1967). "The Zoned Ultramafic Complexes of southeastern Alaska, Part 4III," in *Ultramafic and Related Rocks*. Editor P.J. Wyllie (New York: John Wiley), 96–118.*Geol. Soc. Lond. Spec. Publications*

Teng, F.-Z. (2017). Magnesium Isotope Geochemistry. *Rev. Mineralogy Geochem.* 82, 219–287. doi:10.2138/rmg.2017.82.7

Tian, W., Chen, B., Ireland, T. R., Green, D. H., Suzuki, K., and Chu, Z. (2011). Petrology and Geochemistry of Dunites, Chromitites and mineral Inclusions from the Gaositai Alaskan-type Complex, North China Craton: Implications for Mantle Source Characteristics. *Lithos* 127, 165–175. doi:10.1016/j.lithos.2011.08.013

Tistl, M., Burgath, K. P., Höhndorf, A., Kreuzer, H., Muñoz, R., and Salinas, R. (1994). Origin and Emplacement of Tertiary Ultramafic Complexes in Northwest Colombia: Evidence from Geochemistry and K Ar, Sm Nd and Rb Sr Isotopes. *Earth Planet. Sci. Lett.* 126, 41–59. doi:10.1016/0012-821x(94)90241-0

Valli, F., Guillot, S., and Hattori, K. H. (2004). Source and Tectono-Metamorphic Evolution of Mafic and Pelitic Metasedimentary Rocks from the central Quetico Metasedimentary belt, Archean Superior Province of Canada. *Precambrian Res.* 132, 155–177. doi:10.1016/j.precamres.2004.03.002

Wang, G. Q., Li, X. M., Xu, X. Y., Yu, J. Y., and Wu, P. (2014). Ziron U-Pb Chronological Study of the Hongshishan Ophiolite in the Beishan Area and Their Tectonic Significance. *Acta Petrologica Sinica* 30 (6), 1685–1694.

Wang, X. B., Bao, P. S., and Rong, H. (1996). Rare Erath Elements Geochemistry of the Mantle Peridotite in the Ophiolite Suites of China. *Acta Petrologica Sinica* 11 (Suppl. l), 24–41.

Wang, X. H., Yang, J. G., Xie, X., and Wang, L. (2013). The Genetic Type and Tectonic Significance of Hongshishan Basic-Ultrabasic Rocks in Beishan, Gansu Province. *Northwest. Geology.* 46 (1), 26–55. (in Chinese with English abstract).

Wang, Z. L., Meng, G. X., Tang, H. J., Yuan, L. L., Yang, Z. S, and Xiao, Y. D. (2021). Geochemistry of Clinopyroxene and Chrome Spinel in the Zhaheba Peridotite, Eastern Junggar, Xinjiang, China and Its Chromitite Metallogenesis. *Geology in China* 48 (2), 477–494 [in Chinese with English abstract].

Wei, W. Z. (1978). On the Genesis and Genetic Types of a Chromite deposit in Kansu. *Acta Geologica Sinica* 4, 269–281.

Wei, Z. J. (2004). *Report of regional geological survey of Hongbaoshi Region, China: No. 4 Geological Team of the Gansu Bureau of Geology and Mineral Deposits, scale 1:250,000*. Beijing: China Geological Survey [in Chinese].

Wei, Z. J., Huang, Z. B., Jin, X., Sun, Y. J., and Huo, J. C. (2004). Geological Characteristics of Ophiolite Migmatitic Complex of Hongshishan Region. *Gansu. Northwest. Geology.* 37 (2), 13–18. (in Chinese with English abstract).

Wood, S. A. (1987). Thermodynamic Calculations of the Volatility of the Platinum Group Elements (PGE): The PGE Content of Fluids at Magmatic Temperatures. *Geochimica et Cosmochimica Acta* 51, 3041–3050. doi:10.1016/0016-7037(87)90377-2

Xia, L. Q., Xia, Z. C., Xu, X. Y., Li, X. M., Ma, Z. P., and Wang, L. S. (2005). Relationships between Basic and Silicic Magmatism in Continental Rift Settings: A Petrogeochemical Study of Carboniferous Post-collisional Rift Silicic Volcanics in Tianshan,NW China. *Acta Geologica Sinica* 79 (5), 633–653. (in Chinese with English abstract).

Xiao, W. J., Mao, Q. G., Windley, B. F., Han, C. M., Qu, J. F., Zhang, J. E., et al. (2010). Paleozoic Multiple Accretionary and Collisional Processes of the Beishan Orogenic Collage. *Am. J. Sci.* 310, 1553–1594. doi:10.2475/10.2010.12

Yang, H. Q., Li, Y., Zhao, G. B., Li, W. Y., Wang, X. H., Jiang, H. B., et al. (2010). Character and Structural Attribute of the Beishan Ophiolite. *Northwest. Geol.* 43 (1), 26–36. (in Chinese with English abstract).

Yue, Y., Liou, J. G., and Graham, S. A. (2001). Tectonic Correlation of Beishan and Inner Mongolia Orogens and its Implications for the Palinspastic Reconstruction of north China. *Memoir Geol. Soc. America*, 101–116. doi:10.1130/0-8137-1194-0.101

Zhao, R. S., Zhou, Z. H., Mao, J. H., and Zhao, Z. X. (1994). Plate Tectonic Units and Tectonic Evolution in Gansu. *Reg. Geology. China* 13 (1), 28–36.

Zhou, M. F., and Bai, W. J. (1992). Chromite deposits in China and their origin. *Mineralium Deposita* 27, 192–199.

Zhou, M.-F., Robinson, P. T., Malpas, J., and Li, Z. (1996). Podiform Chromitites in the Luobusa Ophiolite (Southern Tibet): Implications for Melt-Rock Interaction and Chromite Segregation in the Upper Mantle. *J. Pet.* 37, 3–21. doi:10.1093/petrology/37.1.3

Zhou, M.-F., Robinson, P. T., Su, B.-X., Gao, J.-F., Li, J.-W., Yang, J.-S., et al. (2014). Compositions of Chromite, Associated Minerals, and Parental Magmas of Podiform Chromite Deposits: the Role of Slab Contamination of Asthenospheric Melts in Suprasubduction Zone Environments. *Gondwana Res.* 26, 262–283. doi:10.1016/j.gr.2013.12.011

Zuo, G. C., Zhang, S. L., He, G. Q., and Zhang, Y. (1990a). Early Paleozoic Plate Tectonics in Beishan Area. *Scientia Geologica Sinica* 4, 305–314. (in Chinese with English abstract).

Zuo, G. C., Zhang, S. L., Wang, X., Jin, S. Q., He, G. Q., Zhang, Y., et al. (1990b). *Plate Tectonics and Metallogenic Regularities in Beishan Region*. Beijing: Peking University Publishing House. (in Chinese with English abstract).

Zuo, G., Zhang, S., He, G., and Zhang, Y. (1991). Plate Tectonic Characteristics during the Early Paleozoic in Beishan Near the Sino-Mongolian Border Region, China. *Tectonophysics* 188, 385–392. doi:10.1016/0040-1951(91)90466-6

Conflict of Interest: The authors declare that the research was conducted in the absence of any commercial or financial relationships that could be construed as a potential conflict of interest.

Publisher's Note: All claims expressed in this article are solely those of the authors and do not necessarily represent those of their affiliated organizations, or those of the publisher, the editors and the reviewers. Any product that may be evaluated in this article, or claim that may be made by its manufacturer, is not guaranteed or endorsed by the publisher.